



Minnesota State University, Mankato
Cornerstone: A Collection of Scholarly
and Creative Works for Minnesota
State University, Mankato

All Graduate Theses, Dissertations, and Other
Capstone Projects

Graduate Theses, Dissertations, and Other
Capstone Projects

2022

Optimal Speed Control of Electric Vehicles in Traffic with Wireless Charging

Amina Jemi
Minnesota State University, Mankato

Follow this and additional works at: <https://cornerstone.lib.mnsu.edu/etds>



Part of the [Electrical and Computer Engineering Commons](#)

Recommended Citation

Jemi, A. (2022). Optimal speed control of electric vehicles in traffic with wireless charging [Master's thesis, Minnesota State University, Mankato]. Cornerstone: A Collection of Scholarly and Creative Works for Minnesota State University, Mankato. <https://cornerstone.lib.mnsu.edu/etds/1203/>

This Thesis is brought to you for free and open access by the Graduate Theses, Dissertations, and Other Capstone Projects at Cornerstone: A Collection of Scholarly and Creative Works for Minnesota State University, Mankato. It has been accepted for inclusion in All Graduate Theses, Dissertations, and Other Capstone Projects by an authorized administrator of Cornerstone: A Collection of Scholarly and Creative Works for Minnesota State University, Mankato.

Optimal Speed Control of Electric Vehicles in Traffic with Wireless Charging

By

Amina Jemi

A Thesis Submitted in Partial Fulfillment of the

Requirements for the Degree of

Master of Science

In

Electrical Engineering

Under the Supervision of Dr. Vincent Winstead

Minnesota State University, Mankato

Mankato, Minnesota

April 2022

This thesis has been examined and approved by the following members of the committee.

Prof. Vincent Winstead
Advisor

Dr. Jianwu Zeng
Committee Member

Dr. Qun (Vincent) Zhang
Committee Member

ACKNOWLEDGMENT

To begin, I would want to express my gratitude to Dr. Vincent Winstead for his continuing support of my research, as well as for his perseverance, passion, excitement, and breadth of knowledge regarding power converter and control systems. He aided me in comprehending the inductive converter and traffic management system, as well as provided continuous guidance and suggestions. Without him, this expedition would be impossible to complete. Then, I would like to convey my gratitude to the members of my committee. Moreover, I would like to express my appreciation to Minnesota State University, Mankato, for providing me with the chance to pursue my graduate degree. I like to express my heartfelt appreciation to the electrical and Computer engineering and technology department at Minnesota State University for providing me with the required equipment and electrical devices for conducting the study.

Table of Contend

Table of Contents

ACKNOWLEDGMENT	3
Table of Contend	4
List of Acronyms	5
List of Tables	6
Table of Figures.....	7
Abstract:	9
Chapter 1: Introduction	10
1.1 Background	10
1.2 Electric Vehicle and Wireless Power Transfer.....	11
1.3 Electric vehicle charging System	13
1.4 Types of Wireless Charging	15
1.5 Comparison between Wireless Charging over Plug-in Charging:	15
1.6 Inductive Charging.....	16
1.7 The elements of wireless power transfer systems for EVs are as follows:	17
1.8 Wireless Charging Coil Design.....	18
1.9 Wireless charger coil type	19
1.10 Ferrite Shapes	20

1.11 Power Electronics Converter for Electric vehicle	20
1.11.1 Converter on the primary side	20
1.11.2 Converter on the Secondary Side	21
1.12 Compensation Topology	22
1.13 Disadvantages of Static Charging compared with Dynamic Charging	23
Chapter 2: A Literature Review on Inductive Power Transfer for Electric Vehicle.....	24
2.1 The inductive OLEV charging system consists of the following:.....	24
2.2 Misalignment and charging efficiency	25
2.3 Continuous and discontinuous charging lane	25
2.4 Comparison with IPT and without IPT for Dynamic Vehicle:	26
2.5 Online Electric Vehicle Power and efficiency:	27
2.6 Cost-effective coil design.....	28
2.7 Using multiple receiving coils and switching on/off of coils to achieve better efficiency:	29
2.8 Cost estimation:	29
2.9 Intelligent Traffic Management.....	31
Chapter 3 Misalignment of Dynamic Charging	33
3.1 Fundamentals of Design Analysis for inductive Power transfer	33

3.1.1 Basic equations for Power transformer	33
3.2 Coil alignment for Power transfer	34
3.3 Mutual induction calculation.....	35
3.4 Charging structure for dynamic online electric vehicle:	35
3.5 Investigating Misalignment for one vehicle	36
Chapter 4. Simulation setup and result.....	40
4.1 Dynamic charging with one controlled vehicle and one vehicle in the front	40
4.2 Control horizon, Time, and Power consumption of the controlled vehicle	42
4.3 Dynamic charging with one controlled vehicle and one vehicle in the front and one in the back.....	43
4.4 Proposed Dynamic Electric Vehicle infrastructure for Maverick Shuttle.....	45
5. Research Findings and future suggestions	48
5.1 Findings:	48
5.2 Future Work	48
Appendix A:	49
Appendix B:	49
Bibliography.....	52

List of Acronyms

- BEV: Battery electric vehicles
- DAB: Dual Active Bridge
- DWPT: Dynamic Wireless Power Transfer
- EV: Electric Vehicle
- EVI: Electric Vehicle Initiative (EVI),
- HEV: Hybrid electric vehicles
- ICE: Internal Combustion Engine
- IEA: International Energy Agency
- IPT: Inductive Power Transfer
- KAIST: Korea Advanced Institute of Science & Technology
- LPAA: Lima Paris Action Agenda
- OBC: On-Board Converter
- OLEV: Online Electric Vehicle
- PFC: Power Factor Correction (PFC)
- PHEV: Plug-in hybrid electric vehicles
- WPT: Wireless Power Transformation

List of Tables

Table 1: Summary of Current Wireless EV Charging Projects

Table 2: Charging coverage without IPT

Table 3: Charging coverage with IPT

Table 4: The manufacturing cost of OLEV passenger vehicles should be less than that of the hybrid cars and even regular cars with IC engines when they are produced in economical lot sizes.

Table 5: Power consumption for the controlled vehicle for different control horizon values and time for calculation (MATLAB).

Table of Figures

Fig 1: Inductive Power Transfer Sample Prototype

Fig 2: Dynamic Wireless Charging technology

Fig 3: Development of Charging Technology

Fig 4: Different types of Ferrite Shape

Fig 5: General Configuration of the Converter on the Primary and Secondary Sides

Fig. 6: The Different Types of Compensation Circuits

Fig 7: Simplified model for dynamic charging of Electric Vehicle

Fig 8: The Power and efficiency of the OLEV

Fig 9: Selective Switch turn on/off for dynamic charging

Fig 10: Comparison of the cost for infrastructure for PEV (plug-in all battery electric vehicle), OLEV, PHEV (plug-in hybrid electric vehicle), and HEV (hybrid electric

Fig 11: Feedback to maximize inductive power transfer

Fig 12: Generic Diagram of WPT

Fig 12: lateral and angular misalignment

Fig 13: (a) Two coaxial cylindrical helix coils. (b) Two cylindrical helix coils with lateral and angular misalignment.

Fig 14: Lateral and angular misalignment output curve

Fig 15: Energy consumed by the controlled vehicle while traveling.

Fig 16: Velocity of controlled vehicle and vehicle in front (top), and distance traveled by the controlled vehicle and vehicle in the front.

Figure 17: Acceleration of the controlled vehicle and the mutual distance between the two vehicles.

Fig 18: Power consumption by the controlled vehicle

Fig 19: Vehicle velocity and traveling trajectory

Fig 20: Controlled vehicle acceleration and mutual distance

Fig 21: Energy transfer per coil vs speed

Fig 22: MNSU proposed dynamic electric vehicle route

Optimal Speed Control of Electric Vehicles in Traffic with Wireless Charging

Amina Jemi

A THESIS SUBMITTED IN PARTIAL FULFILLMENT OF THE
REQUIREMENTS FOR THE DEGREE OF
Master of Science

In

Electrical Engineering

MINNESOTA STATE UNIVERSITY, MANKATO
MANKATO, MINNESOTA
April 2022

ABSTRACT

With the increase in electric vehicle use in recent years and expected increase in the future, a wireless network provides a possible option to allow vehicles with a route while maintaining an approximate net-zero energy balance under certain scenarios. In this type of network, a collection of wireless charging pads is installed under the road, and energy transfer occurs, while a vehicle with wireless charging capability is driven over the charging pads. This thesis describes a methodology and modeling to solve an optimization problem involving a speed-controlled vehicle in traffic. The methodology incorporates a receding horizon dynamic model with constraints. Suboptimal results are described under multiple traffic scenarios. Several scenarios are explored while the vehicle under constrain (controlled vehicle) is dynamic, its charging behavior with being the only vehicle on the route and while the vehicle is following the route while other vehicles present on the route and the controlled vehicle is following the traffic. Besides, describe the methodology for dynamic charging and the optimal charge station for the current charging rate. This model of predictive control can be adopted in real-time given certain information is available for the controlled vehicle and traffic conditions.

Chapter 1: Introduction

This chapter presents the framework of the thesis, which includes a background of electric vehicles, their evolutions, types, and importance. It also discussed various charging methods and topologies for electric cars and wireless electric vehicles. Moreover, the dynamics of energy storage and converters for electric vehicles and their socio-economic changes are delineated.

1.1 Background

Non-renewable energy resources such as gas, oil, coal, and nuclear reactants are the conventional energy resources that have widely accepted technology for electricity generation and transportation. The reasons behind this are the comparatively lower investment cost, flexible mode of operation, and ease of connection with the grid. Fossil fuel formation is a natural and geological process, and it is formed from fossilized remains of plants by pressure and heat. However, these resources are limited and will be exhausted soon, as these resources have been massively used in the last century; fossil fuel generated in 1900 was 5,973 terawatts, whereas, in 2019, it was 135,809 terawatts. In the United States, fossil fuel generation was 2,001.88 terawatts in 1900, whereas in 2014, it went to 21,353.8 terawatts [1].

These non-renewable resources emit greenhouse gases like carbon dioxide and methane, which trap the sun's heat in the atmosphere, causing global warming and disrupting land and marine life. Greenhouse gases are the cause of the increase in the global temperature

as we have seen the global temperature has risen 0.8 degrees Celsius (1.4 degrees Fahrenheit) since 1880[2] [3]. It also causes an increase in the acidity of ocean water (305 increase since 1750) which is detrimental to ocean animals [1]. Moreover, greenhouse gases increase the temperature which stresses and decreases plant growth and bake the soil; therefore, less plant growth and wildfire have become more common. Climate change harms every aspect of human life. Only air pollution-related death worldwide is 3.61 million, wherein in the United States, the number is 243,609 in 2015[9].

Among the transportation, industrial, residential, and commercial energy sectors, the transportation sector is responsible for the highest CO₂ emission in the USA [2]. Conventional vehicles emit many harmful gases, including CO₂, which increase the greenhouse effect. Road vehicles such as cars, trucks, busses, and two and three-wheelers are responsible for about 75% of the total transportation emission, and transportation accounts for 24% of the direct CO₂ emission [3]. The CO₂ emission has been slowing down since 2007; however, the transportation sector is still leading every other industry. We are looking for renewable energy resources such as wind and solar integration and electrification of the transport section. The world is seeing a current trend of rising renewable energy resources. According to the International Energy Agency (IEA), the net renewable energy capacity would be 4% higher in 2020 than the previous year, which means the world will see a 198GW renewable energy installation that will break all the previous records [7]. Due to the Covid-19 situation, the growth of renewable energy has slowed down but did not stop growing in 2021[7].

To promote the rapid adoption of green renewable energy sources, electrification of vehicles has been advocated worldwide. Because of continuous research and development, an increase in the global sale of Electric vehicles and a decrease in the size of battery packs and vehicle prices is achieved [61]. Fig 1 shows the increasing number of electric vehicles purchases worldwide which is a rapid growth trend. The IEA supports and coordinates the Electric Vehicle Initiative (EVI), a multi-government policy working toward the adoption and acceleration of electric vehicles worldwide. EVI calls to action in June 2021 at the 12th Clean Energy Ministerial to close the gap between EV sales in 2030. EVI and IEA are working to fulfill their transport focus on Lima Paris Action Agenda (LPAA) and Paris agreement. They are calling for the deployment of a 20% share of all road transport vehicles by 2030, adding more than 100 million Electric vehicles [62]. Countries and world leaders are coming forward to achieve the goal; the United States has planned to operate a grid powered by a zero-carbon power plant and achieve a very low-cost zero-carbon on-road vehicles and transit system [63]. Besides, increasing the jobs in this sector is also a target of the US government [64]. Moving towards electric vehicles will fulfill the target of decreasing greenhouse gas emissions, checking future climate shifts, and ensuring reliable, timely, and cost-efficient energy delivery. An advanced transportation system infused with electric vehicles will have significant benefits for energy security. Recently, the leading Inductive Power Transfer (IPT) technology providers in electric cars, buses, and trains such as Bombardier and Halo IPT reported maximum efficiencies up to 95% [11].

1.2 Electric Vehicle and Wireless Power Transfer

Electric vehicles are not a new concept. The first electric car was invented sometime between 1832 and 1839. In November 1881 Gustave Trouve presented an electric car at the Exposition International d Electricite de Paris. One of the early electric cars was built by Thomas Parker [4], and in 1912 Thomas Edison created an electric car [5].

The initial presentation of Maxwell's equation is considered the precursor of WPT and can be traced back to 1862, however, the most prominent history of wireless power transfer officially began in 1891[65], when Nikola Tesla built his famous Tesla coil, also known as the magnifying transmitter. The system comprises two loosely coupled and tuned resonant circuits: a primary circuit and a secondary circuit. The coils were built with many single-layer solenoids, which significantly lowered coil resistance while simultaneously boosting the quality factor. Nikola Tesla never commercialized his project due to its perceived risk, low efficiency, and budgetary constraints [67] [68]. Electromagnetic waves have been utilized for wireless communications and distant sensing applications, among other things since Nikola Tesla's earliest tests. In recent years, advances in semiconductor technology have made Tesla's vision a reality. A transmitter device generates an electric field by receiving electricity from the power source and a receiver device receives power and transfers it to the load.

Researchers from Auckland University have been working on wireless charging for electric vehicles since 1990, they have developed a 213-meter-long test track with two 120-meter-long powered sections built from the ground up. The system's overall efficiency was estimated to be around 60% [68].

WPT has been studied at the Korea Advanced Institute of Science & Technology (KAIST), with a focus on Dynamic Wireless Power Transfer (DWPT). Several designs of the On-Line Electric Vehicle (OLEV) have been proposed since 2009, each based on changes to previous designs. The 5th generation OLEV was created by KAIST [69]. At a frequency of 10 kHz, 3 kW could be carried over a 1 cm air gap, resulting in an 80 percent system efficiency. The vehicle was mechanically set to a maximum lateral misalignment of 3 mm [66] [67]. The 2nd Generation E-Bus, which had a maximum air gap length of 17 cm, was used at KAIST on-campus bus services. Ten I-type pickup coils were installed beneath the bus and each of these pickup coils is capable of handling 6 kW, and it used a U type supply rail instead of an E type supply rail. When transmitting 60 kW, the system's highest efficiency was 72 percent. A 23-centimeter increase in lateral misalignment tolerance was achieved while maintaining 70 percent of maximum power output. In addition, the operating frequency has been raised to 20 kHz [44] [65].

Table 1 below summarizes the advancement of stationary and dynamic electric vehicles which is an important topic for the thesis since dynamic charging vastly depends on the development of power rating for the transformer coil of EV. The paper will focus on dynamic electric vehicles and draw some conclusions in the later chapter where the research from KAIST is used as a reference resource.

Institute / corporation	Year of Installation	Location	Project Type	Vehicle Type	Power	Air Gap	Efficiency
Auckland University & Conductix-Wampfler	1997	Auckland	Public Demonstration (Stationary)	5 Golf buses	20kW	50mm	90-91%
	2002-2003	Italy		8-23 mini buses	60kW	30mm	-
Auckland University & Qualcomm Halo	2010	Auckland	Evaluation kits (Stationary)	Private vehicles	3kW	180mm	85%
	2012	UK	Public Demonstration (Stationary/Dynamic)	-	-	-	-
ORNL	2010	US	Prototype (Dynamic)	-	4.2kW	254mm	92% (coil-to-coil)
	2012	US	Prototype (Stationary)	-	7.7kW	200mm	93% (coil-to-coil)
	2012	US	Prototype (Stationary/Dynamic)	GEM EV	2kW	75mm	91% (coil-to-coil)
KAIST	2009	Korea	Prototype (Dynamic)	Golf Bus	3kW	10mm	80%
				Bus	6kW	170mm	72%
				SUV	17kW	170mm	71%
	2010	Korea	Public Demonstration (Dynamic)	Tram	62kW	130mm	74%
2012	Korea	Bus		100kW	200mm	75%	
MIT WiTricity & Delphi	2010	US	Commercial kits (Stationary)	Private vehicles	3.3kW	180mm	90%
Evatran	2010	US	Commercial Product (Stationary)	Private vehicles	3.3kW	100mm	90%

Table 1: Summary of Current Wireless EV Charging Projects [54]

1.3 Electric vehicle charging System

Electric vehicles are generating more attention recently because of their performance potential rapid growth in the future, even though the charging mechanism still can be considered under developing conditions. Numerous factors such as rapid charging, optimal infrastructure design, fewer converter, compensating components, and safety features are

significant concerns for rapid development. The charging technology of electric vehicles is primarily divided into two types [39].

1. Wired charging
2. Wireless charging.

Wired Charging based on the type of energy used: Wired Charging vehicles is the most common technology of charging and can be grouped into three groups based on the type of energy used to power them. They are followed,

(I) Hybrid electric vehicles (HEVs): HEVs are equipped with a small electric battery and an internal combustion engine (ICE) that can run on electricity and gasoline. Due to the absence of an external charging port on HEVs. The electric battery can be charged exclusively through the vehicle's (regenerative) braking system and ICE [52] [58].

(II) Plug-in hybrid electric vehicles (PHEVs): (PHEVs) have an external socket (plug) and a larger battery. The battery is charged externally via the plug and internally via the regenerative braking system [59].

(III) Battery electric vehicles (BEV): BEVs are electric vehicles with no internal combustion engine. Only the external socket is used to charge the electric battery.

Wired Charging based on input type: Based on the input voltage, wired charging can be categorized as follows:

AC charging: AC charging is often accomplished using an On-Board Converter (OBC), which converts the alternating current(AC) to a direct current(DC).AC charging can be separated into two categories.

(I) Single-phase slow charging: On board, slow charging makes use of a multi-stage converter to provide low voltage ripple as well as a high-power rating [12]. However, it is subject to higher costs, weight, and board space [16] [17], resulting in additional components. An ac/dc converter rectifies the grid voltage, which is then sent to a power factor correction (PFC), and the output of the PFC is transmitted to an intermediate DC link bus and an isolated DC-DC converter, which in turn offers a safe battery charging [17].

(II) Three-phase fast charging:

DC charging: DC charging is further divided into the categories listed below.

(I) Off-Board Fast Charging: Due to the existence of a rectifying unit in the charging station, such technologies can effectively charge the battery of a BEV without using a charging cable. As a result, they can minimize the total size and weight of the driving vehicle. For these specific charging technologies, DAB topologies are the most prevalent. These charging technologies are noted for their quick charging (specifically, charging times of less than 1 hour). The fast charging of electric vehicles was a push toward the dynamic charging which is presented below.

(II) Off-board Rapid Charging:

Rapid charging technologies, which consume more power and charge than traditional fast charging technologies, are an enhanced form of fast charging technologies. The charging period is shorter with various charging methods, and BEV batteries with DC 320 to 500 V can be charged up to 80% in 15 minutes [17]. Off-board Rapid Charging can be considered as the precursor of the dynamic electric charging in which an electric vehicle is charging while driving.

1.4 Types of Wireless Charging

This section discusses different types of wireless charging solutions for electric vehicles.

Wireless charging technologies can be split into three categories based on the distance between them:

1. Near field charging technologies

Near-field charging technologies are those that charge within a few centimeters of the device. The near-field charging technologies include:

- a. Inductive charging
- b. Magnetic-resonant charging
- c. Capacitive charging

2. Medium field charging technologies

Medium-Field Charging technology makes use of mechanical force as a primary energy-carrying medium. They can be implemented in charging applications with a low power range of 1.5 to 3 kW [26] [27].

3. Far-field charging technologies

The far-field charging technologies for BEVs uses electromagnetic radiation (EMR) such as laser charging, microwave charging, and radio wave charging [27] [29].

1.5 Comparison between Wireless Charging over Plug-in Charging:

Wireless charging systems have grown in popularity in recent years due to their advantages over regular plug-in charging. Several advantages might be noted as

- 1) It enables compact, flexible, and safe EV charging without requiring direct human interaction. It can function independently when parked over a charger; it immediately begins charging without any electrical connection.
- 2) Low chance of danger – the wire used in a plug-in system may present a trip hazard to pedestrians; also, because the charging environment in a public setting is frequently adjacent to the road, the possibility of another automobile colliding with someone is not negligible [28].
- 3) The overall charging cost is significantly lower than conventional conductive charging.
- 4) The charging system's layout is simple, making it ideal for residential use with minimal maintenance. Inductive Power Transfer (IPT) systems have wireless charging which is advantageous for individuals who have trouble connecting a charging connector that is substantially larger and heavier than a conventional NEMA-5 plug [28] [30].
- 5) Dynamic WPT technology enables vehicle charging while in motion, thereby increasing EV range.
- 6) Wireless charging in conjunction with vehicle-to-grid (V2G) operation has the potential to significantly reduce the total battery capacity of electric vehicles by up to 20% [10]. The performance of wireless charging can be boosted by up to 90% by selecting the appropriate coil pair, duty cycle, and switching frequency [30].
- 7) Weatherproof - Because IPT systems can be installed underground, they are not exposed to wet, snowy, or freezing conditions.

8) Vandalism prevention – Vandalism, such as copper cable theft, is a problem with public plug-in systems. Because potential vandals and thieves cannot see the architecture of the IPT system, they are unlikely to dig beneath the road to steal it

1.6 Inductive Charging

Inductive charging is one of the most cost-effective methods of near field charging and is being widely used for WPT for Electric vehicles. This paper will mainly focus on inductive charging for the following chapters of this paper. For the electric vehicle power transfer from a transmitting pad to a receiver pad via an electromagnetic field, optimizing power transfer while maintaining a high-efficiency level is crucial for these systems' design and operation. Additionally, regulating the EV power bus voltage is necessary to ensure long battery life. This can be performed by regulating both the switching frequency and conversion ratio of the primary-side converter (such as a high-frequency AC-AC converter at the transmitter pad) and the secondary-side converter concurrently (such as a full-bridge, dual-active Bridge DC-DC converter at the receiver pad). While WPT systems have become prevalent in various BEV applications, they continue to face several challenges, including power pad and coil design, electromagnetic field protection, high-frequency power converters, and metal object detection. These charging solutions have a power transfer capacity of 3 to 60 kW across a short distance of 4 to 10 cm, with a maximum efficiency of 90% over that distance [27] [28]. If the vehicle being charged is stationary, it is referred to as "battery electric vehicle (BEV) charging" or "static charging," whereas if the vehicle is moving, it is referred to as dynamic charging or online electric vehicle

(OLEV). In the OLEV setup, the primary coil is embedded in the pavement at spaced locations, establishing a charging roadbed that allows power transfer at several spaced locations throughout the roadbed [52]. Fig 1 below illustrates an example of a prototype design.

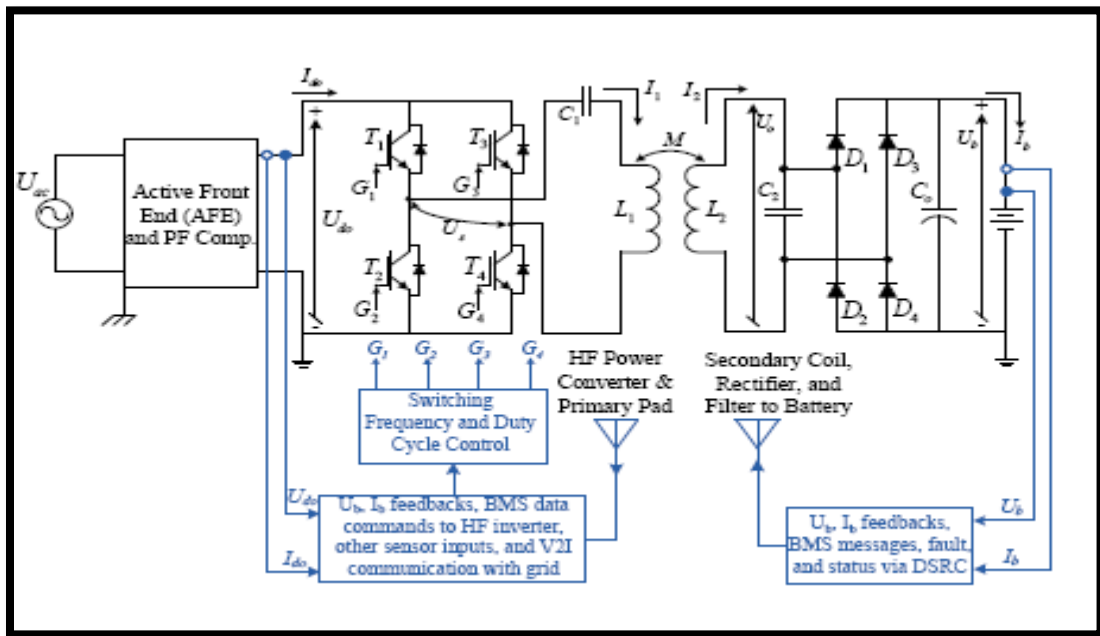


Fig 1: Inductive Power Transfer Sample [30]

1.7 The elements of wireless power transfer systems for EVs are as follows:

1. Energy source: An energy source can be either grid-connected or linked with a renewable energy source, such as a solar or wind system.
2. Electromagnetic field transmission system: Electricity is transported by an electromagnetic field. The power transfer is based on Faraday and Lenz's law, which states that when a conductor is supplied with a time-varying current, a magnetic field is generated around it.

3. Energy collection system: The energy collection system collects energy via the induced current on the secondary conductor created by the time-varying magnetic flux and transmits it to the vehicle's battery or motor [43].

Figure 2 below shows how the dynamic vehicle gets power from the pad underneath the road.

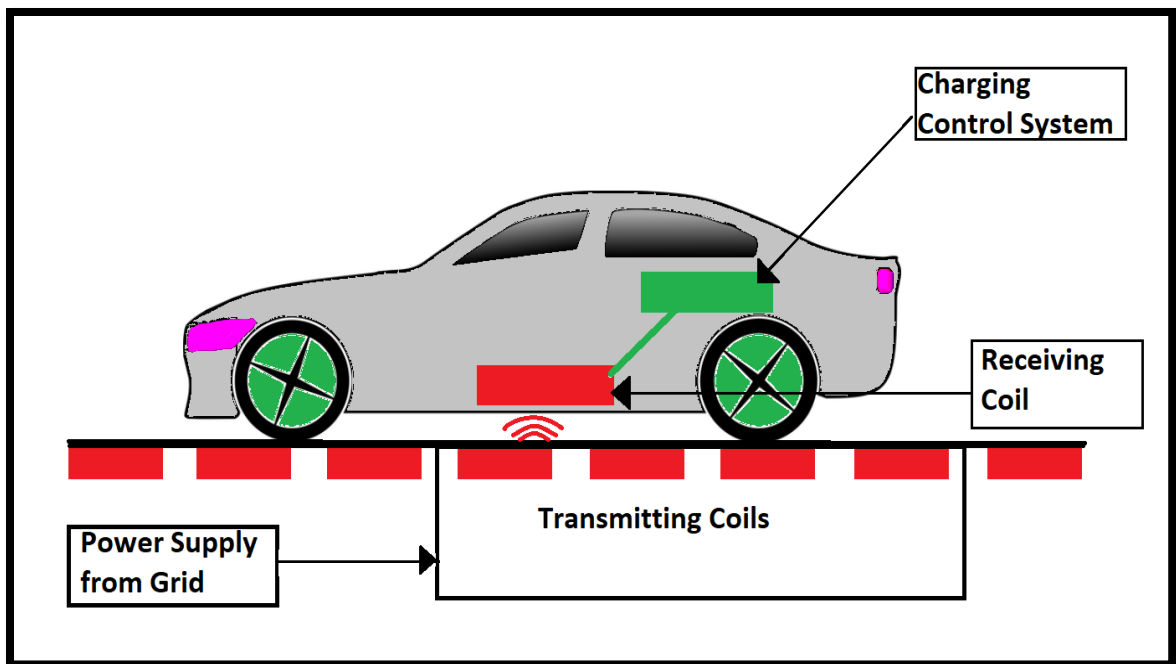


Fig 2: Dynamic Wireless Charging technology

1.8 Wireless Charging Coil Design

Without the contact provided by the cable and plug in the WPT system, the shape, size, and position of the magnetic core material and coil windings contribute significantly to wireless charging performance, including charging distance, power level, and transmission efficiency. Electric current travels through the primary coil, creating a magnetic field that varies in time. The secondary coil intercepts the magnetic field in the region of the primary

coil, thereby inducing a voltage. The quantity of induced voltage is proportional to the length of the air gap between these coils, the number of turns, and the time derivative of the magnetic field. Induced current passes through the secondary coil because of this voltage. The coils create a loosely coupled transformer connected via the primary flux channel, including leakage that does not contribute to power transfer. By connecting each coil to the compensation network, it is possible to maximize the current flowing through the coils due to resonance. For both stationary wireless EV charging and dynamic Power EVs, the primary transmitting side is often stationary beneath the ground [10][11]. The primary side's power transmission unit might be either an extended conductor (referred to as a track) or a lumped coil pad (to deliver power at discrete locations for stationary EV charging and dynamic charging). On the other hand, the secondary receiving side of an EV is placed at the bottom and is intended to capture the transferred power and can be constructed in various topologies using a lumped coil pad [20].

1.9 Wireless charger coil type

Coils are a critical component in magnetic field-based wireless power transfer. Magnetic flux is guided using ferromagnetic cores [71]. With increasing temperature, the efficiency decreases due to Ohmic losses and ferrite material losses. Litz wire is used to minimize the loss of skin effect. DD, DDQ, Bipolar pad, Tripolar pad, and zigzag pad are the new form pads. Circular and square transmitting coils are two common topologies for EV static wireless charging systems. DD quadrature coils (DDQ) are primarily used on the secondary side of electric vehicles (EV). The length of the DDQ pad wires is twice that of the wires

used in circular coils [22] [23]. Figure 3 below illustrates various coil and ferrite topologies suitable for stationary and dynamic electric vehicle charging.

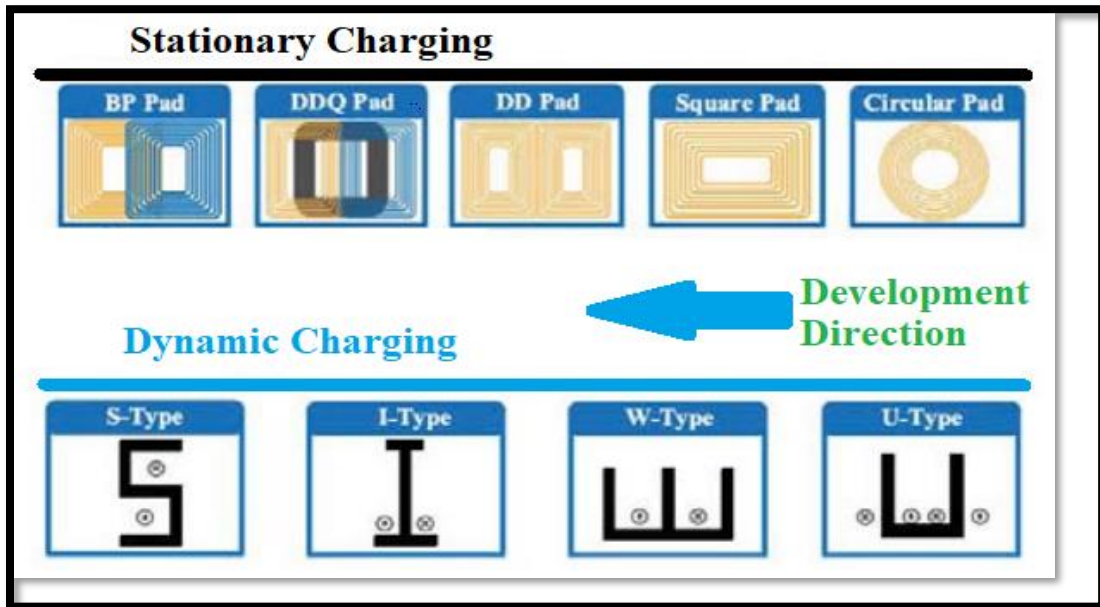


Fig 3: Development of Charging Technology [22]

1.10 Ferrite Shapes

The main factors in designing a ferrite core are size and shape constraints, frequency operating range, permeability, and cost-effectiveness [22]. Accuracy in the design of magnetic ferrite core will redirect the path of magnetic fluxes from the transmitter side to the receiver side. It has a significant effect on improving the mutual inductance and self-inductance of the coils—different types of ferrite shapes used in electric vehicle dynamic charging applications [21] [23]. Figure 4 below shows the different types of the ferrite core.

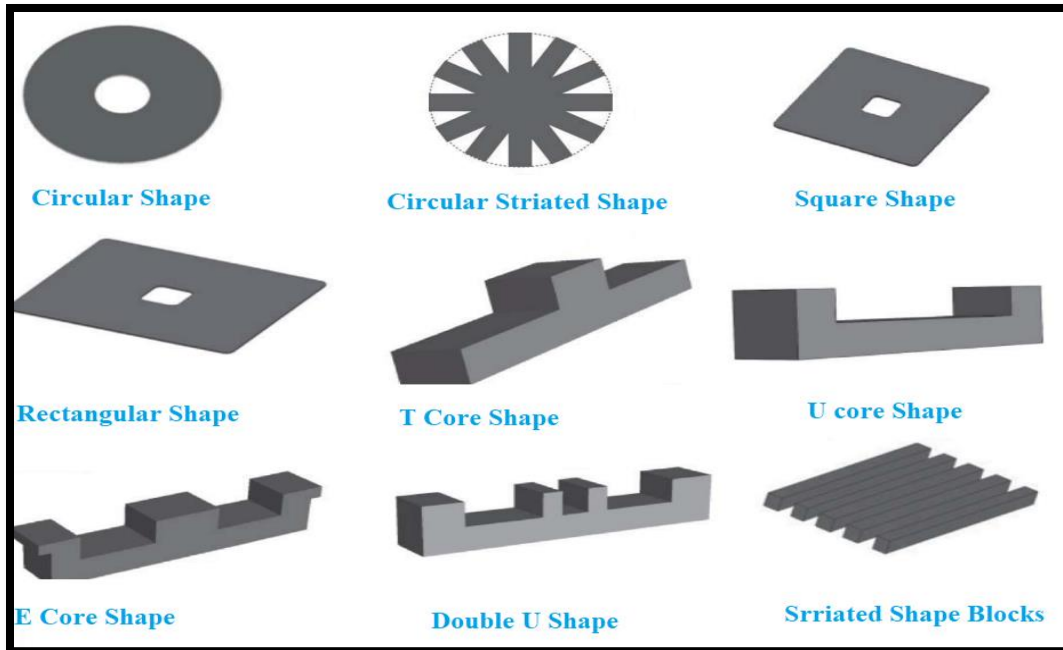


Fig 4: Different types of Ferrite Shape [23]

1.11 Power Electronics Converter for Electric vehicle

Four conversion steps are required for the power electronic converters used in a typical grid-to-vehicle DWPT system. These include front-end converters and high-frequency inverters on the primary side, while on the secondary side, rectifiers, and back-end DC-DC converters are used.

1.11.1 Converter on the primary side

Converters on the Primary Side Front-end converters often contain grid-side rectifiers, power factor correction (PFC), and other DC-DC converter stages among primary converters. The converters can be a straightforward buck, boost, or buck-boost converters, with the buck DC-DC converter most common. Controls from the front-end converters

assist in maintaining an operating point for the DWPT stages, which aids in their soft switching. In DWPT, the most common inverter configurations include voltage-fed single-phase, three-phase, or multiphase inverters and current-fed push-pull and class EF structures. These inverters are used in DWPT systems to drive single or multiple coils and provide a variety of methods for controlling the switching of the appropriate pads.

1.11.2 Converter on the Secondary Side

Diode rectifiers dominate secondary-side converters, with many works attempting to keep the secondary side as basic as feasible. Synchronous rectification can be used to enhance efficiency at the expense of control. Numerous secondary-side controlled DWPT systems incorporate a second DC-DC converter after the rectifier. These typically include buck or buck-boost converters for rectifiers driven by current while connected in series LC components. Boost or buck-boost converters are used for rectifiers driven by voltage usually with a parallel compensated LC circuit on the secondary side. Numerous rectifying stages are frequently used in conjunction with DDQ-type coils or multiple secondary pads, but they are not widely used because they add bulk to the vehicle. The basic rectification is shown below in figure 5.

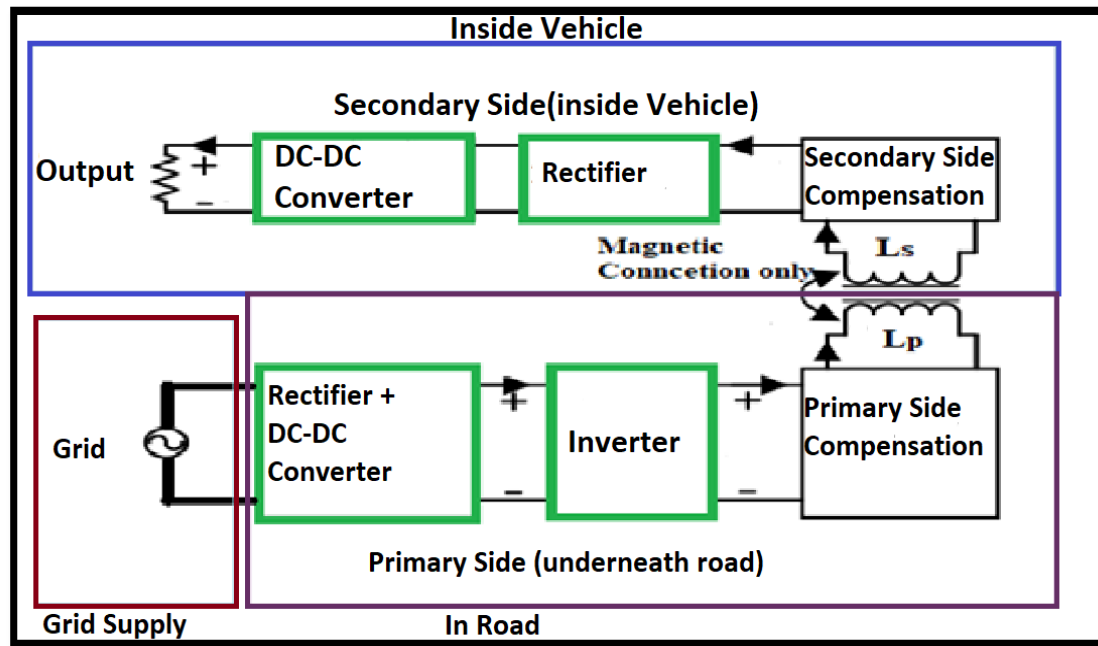


Fig 5: General Configuration of the Converter on the Primary and Secondary Side

1.12 Compensation Topology

A compensation circuit is also required due to the low power transmission due to the high leakage inductance created by the air gap between the ground and the vehicle. Compensation also results in increased power transfer capabilities while minimizing device stress. The advantage of LC resonators is that they provide greater control during the design phase. Compensator capacitors can be connected in series or parallel to the coil in the LC resonator. Due to the shifting load and variable coupling coefficient encountered during the EV charging process. Series-Series (SS) and Series-Parallel (SP) topologies offer better performance in constant frequency WPT battery charging.

The SS topology is more efficient and operates across a more comprehensive load resistance range than the SP topology [21]. S-S compensation enables significant VA input, high power transmission over a long distance, high alignment tolerance, the low impedance at the resonant stage, and low-frequency tolerance on efficiency. Additionally, S-P compensation provides a high VA input suited for EVs, a high-power transfer capability over a long distance, a high alignment tolerance, a low impedance at the resonant stage, and a low-frequency tolerance on efficiency.

Parallel-Series and Parallel-Parallel configurations are not suitable for EVs because they provide low VA input and low output voltage. Fig 6 below shows different types of compensations that are used for both primary and secondary sides.

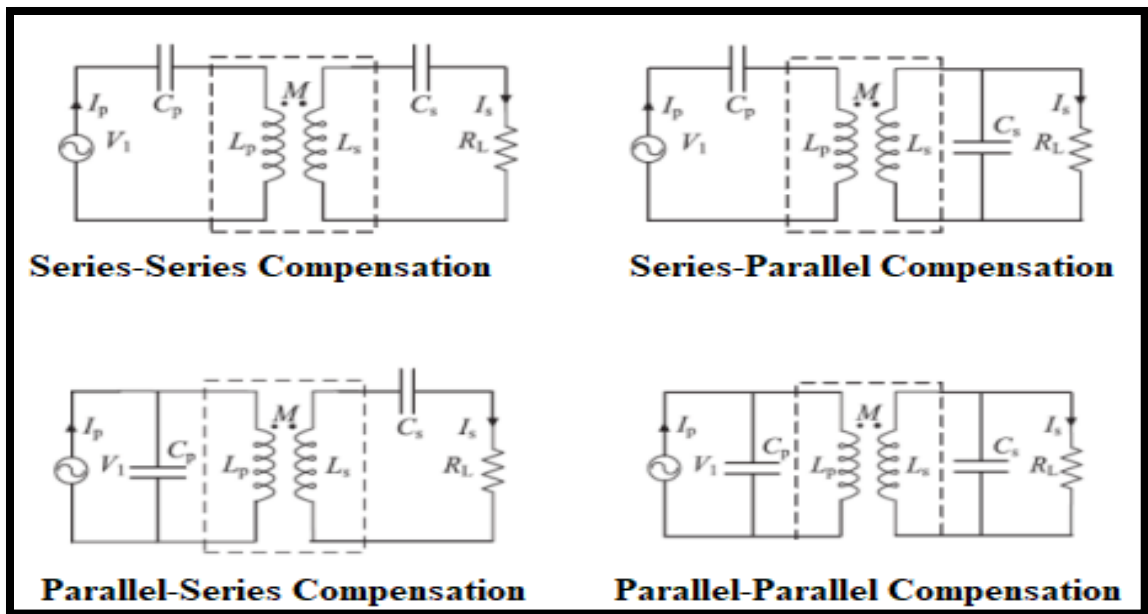


Fig 6: The Different Types of Compensation Circuits [21]

1.13 Disadvantages of Static Charging compared with Dynamic Charging

There are several significant disadvantages to current Li-ion batteries, including the following [25] [26]:

1. Their low energy density (200 Wh/kg compared to 12,000 Wh/kg for petroleum).
2. Their high initial cost (up to S\$1,000/kWh, with a long-term goal of US\$300/kWh).
3. Charge rate limitations due to internal electrochemical processes.
4. Degradation, which limits the acceptance of battery-powered vehicles due to component life being unpredictable.
5. The environmental costs associated with the technology.

On the other hand, charging dynamically can improve the situation as follows:

1. Dynamic Wireless charging technology aims to alleviate range anxiety and boost EV reliability by partially or eliminating overnight charging via a compact network of dynamic chargers positioned along roads that keep the vehicle's batteries charged at all times.
2. By decreasing the size of the battery pack required, dynamic charging can reduce the cost of electric vehicles. If sufficient recharging energy is easily accessible, batteries will not be required to power the vehicle during its range. However, they will instead power the vehicle when the IPT system is unavailable.
3. Depending on the battery's power capacity, dynamic charging may extend the driving range while simultaneously shrinking the battery pack's size [39].

This chapter provided the background for electric vehicles and the development of wireless charging. It also discussed the different types of charging methods and the benefit of wireless charging compared to other methods. This background discussion will provide a better understanding of the following chapters.

Chapter 2: A Literature Review on Inductive Power Transfer for Electric Vehicle

This chapter presents the charging infrastructure for dynamic charging vehicles or online electric vehicles (OLEV), introduces what this thesis proposes for discontinuous charging via a charging pad over a continuous charging lane, and the improvement in transportation systems by using Inductive Power Transfer (IPT). In addition, we consider the parameters like power and efficiency of OLEV, misalignment affecting the efficiency, and efficient coil design for dynamic charge stations. As this thesis considers the optimal speed and its control behavior of the vehicle in traffic, this chapter also introduces the intelligent traffic management system. A simplifying model is shown in figure 7.

2.1 The inductive OLEV charging system consists of the following:

1. A power converter to achieve the 60 Hz AC electricity from the AC grid to road-embedded power tracks. This incorporates a high frequency($\sim 20\text{kHz}$) magnetic field coupling and high power transfer efficiency from the primary to the secondary side with assumed optimal magnetic field coupling and power transfer efficiency from the primary to the secondary side [44]
2. Roadway Infrastructure consists of road-embedded power tracks and several built-in segments along the route; two 200-amp power lines flow in opposite directions to form a loop and generate direct current power for the electric motor. Only the portion beneath the car is turned on to ensure optimal power transfer.

- An electric vehicle equipped with a WPT pick-up coil and appropriate control hardware.

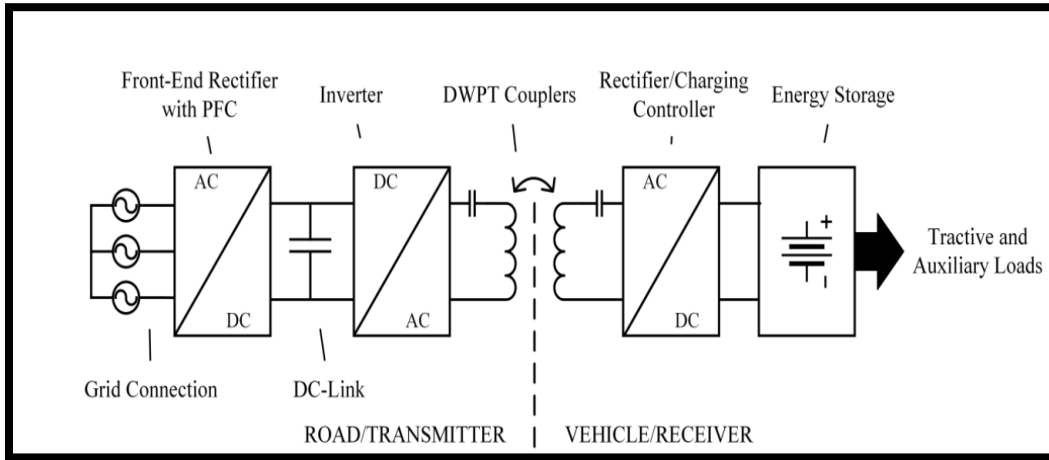


Fig 7: Simplified model for dynamic charging of Electric Vehicle [44]

2.2 Misalignment and charging efficiency

Magnetic misalignment is the cause of the low coupling coefficient and has been extensively studied to demonstrate the theory. Research demonstrates that extending the coil radius from .1m to .25m enhances self-inductance by nearly 66% while maintaining the same misalignment behavior. Additionally, as the coil radius rises, mutual inductance increases by 82.6 percent, whereas misalignment decreases by around 48% [33]. The coupling coefficient increases by approximately 66% as the coil radius increases; however, decreases by approximately 42% in the presence of misalignment. The self-inductance parameter inductance grows by around 11% as the wire radius increases, while the misalignment behavior remains constant. While the mutual inductance is mainly unaffected by the wire radius under identical conditions, it reduces by approximately 62

percent as the misalignment grows. As the wire radius grows, the coupling coefficient changes, reducing by approximately 60% in response to an increase in misalignment [33] [34]. However, the paper did not mention no-cost estimation in any of the scenarios or for a long-distance dynamic charging mismatch.

2.3 Continuous and discontinuous charging lane

A continuous charging lane consumes more electric power than a discontinuous charging lane. However, research showed that discontinuing the wireless charging lane provides better efficiency than the continuous wireless charging trail/lane [36]. With a discontinuous charging, the lane has the highest cumulative total energy output of 2887.509 kW (0.8021 kWh) [36]. This data helps us to answer the question that discontinuous charging pad provides better efficiency and needs less material as a consequence less cost.

2.4 Comparison with IPT and without IPT for Dynamic Vehicle:

Road electrification can increase the driving range for an electric vehicle without worrying about stopping and recharging, even if we can electrify the road partially. Research on three vehicle types (compact car: Honda Insight; large car: Chevrolet Impala; and SUV: Ford Explorer) was considered, equipped with small battery packs (8, 11, and 15 kWh, respectively) and capable of operating in three distinct driving cycles [low-demanding urban driving cycle (UDDS), highway driving cycle (HWFET), and highway driving in a mountainous region (HW-MTN) [39]. The vehicles have a minimum driving range, seldom reaching 50 miles in any direction. The segment of roadway that needs to be enabled for IPT was then calculated to improve the vehicle's range to 300 miles or more. When the

optimization process is applied to minimize the highway length that must be powered, the following table 3 summarizes the results. It is estimated that around 30 kW of power was delivered from the generator to the vehicle and even if only 1% of the route in urban areas is electrified, most vehicle types can quickly meet the 300-meter target range with a relatively small battery pack. From that, it can be said that by using dynamic charging stations on the road we can assure a better and stress-free driving range, and Tables 2 and 3 below show the improvement we can make.

Driving Range Without IPT (in Miles).			
	UDDS	HWFET	HW-MTN
Insight (8 kWh)	38.17	37.14	22.99
Explorer (15 kWh)	36.09	33.00	18.83

Table 2: Charging coverage without IPT [39]

IPT Coverage Required for 300-mi Range (30 kW Delivered to Vehicle).			
	Insight	Impala	Explorer
UDDS			
Coverage (%)	0.46	0.91	1
HWFET			
Coverage (%)	17	27.3	43.8
HW-MTN			
Coverage (%)	17.2	35.4	64.3

Table 3: Charging coverage with IPT [39]

2.5 Online Electric Vehicle Power and efficiency:

Research has been done to show that the distance between the subsurface coil and the bus's power-receiving unit was roughly 17 cm. The most incredible efficiency of electric power transfer was 72 percent, exceeding our design goal of 60 percent for this system. As the distance between the pickup unit and the subsurface coil is reduced or eliminated, the system's efficiency increases [42]. It established a target of installing a battery that would provide a bus with a free driving range of 10 kilometers and a car with 30 kilometers. It concluded that if around 30% of Seoul's roadways are equipped with subterranean electric power coils, most vehicles will be able to navigate the city without recharging their batteries off-road shown in figure 8.

The infrastructure costs of OLEV were compared to those of several alternative electric car systems. The infrastructure cost of OLEV is anticipated to be only 73% of the total infrastructure cost of all battery-powered systems. Additionally, its cost is substantially cheaper than an electric track-trolley system. However, it supplied no details on how they arrived at their conclusion or the general transportation area of the Seoul metropolitan area.

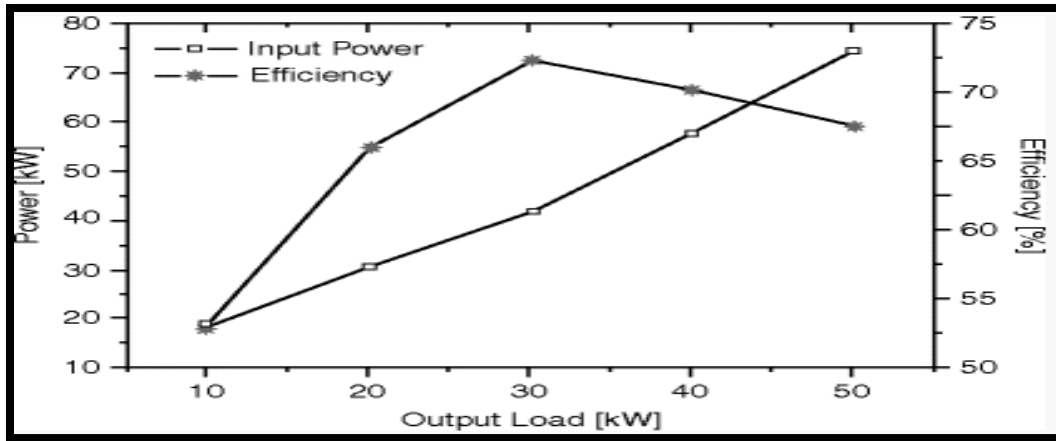


Fig 8: The Power and efficiency of the OLEV [42]

2.6 Cost-effective coil design

Coil design for dynamic wireless power transfer is a crucial point for the efficiency of electric vehicles. The article compares the economics and performance of three distinct types of coil couplers with rectangular, circular, and hexagonal shapes. The raw materials' related WPT performances will be quantified and studied using the same volume of raw materials. This will establish the ideal coil topology for superior characteristics and reduce investment in EV dynamic charging [35] [36]. Both modeling and testing will be utilized to establish the proposed dynamic charging system's validity and cost-effectiveness.

The following findings were drawn from studying the cost-effectiveness numbers for static (aligned position) and dynamic (horizontal misalignment position) pricing scenarios [35] [36]:

1. Due to its higher cost-effectiveness, the rectangular coil can be used as the principal transmitting component for dynamic charging. The rectangular coil, in particular, provides a higher capacity for power transfer at a lower material cost.

2. Due to the improved cost-effectiveness of the hexagonal coil, it can be employed as the principal transmitting component for static charging. On the other hand, due to its capacity to concentrate the output power in a single place, the hexagonal coil can be an auxiliary component for dynamic charging. Circular coils are a cost-effective method of transferring energy. As a result, it is not suggested for system installation to use this coupler type.

2.7 Using multiple receiving coils and switching on/off of coils to achieve better efficiency:

1) Magnetic resonant coupling can be used to transmit energy from a large source coil to one or smaller load coils, with lumped capacitors at the coil terminals providing an easy way to match the coils' resonant frequencies. This mechanism has the potential to be a highly reliable method of wirelessly powering multiple receivers from a single large-source coil. 2) A relatively simple circuit model captures the essential characteristics of the resonant coupling interaction, with parameters derivable from the first principal descriptions, direct measurement, or curve fitting techniques. 3) A critical issue in powering multiple receivers is coupled-mode frequency splitting, which occurs when two receivers are close enough to one another that their magnetic fields are strongly coupled. Control circuitry that tracks resonant frequency shifts and retunes the receiving coil capacitances is one possible solution to this problem [49].

Figure 9 shows that the sensors on all of the transmitting coils will be activated as a result of the communication that has been received. The relays that are connected to each of the transmitting coils, on the other hand, are not open. Only when the electric vehicle (EV)

approaches the transmitting coil L_1 , will the sensor signal the contact of the relay S_1 to turn on, and the transmitting coil L_1 will be powered, resonating with the receiving coil and transmitting energy wirelessly to the electric vehicle. In the meantime, transmitting coil L_2 is ready to begin transmitting signals [31].

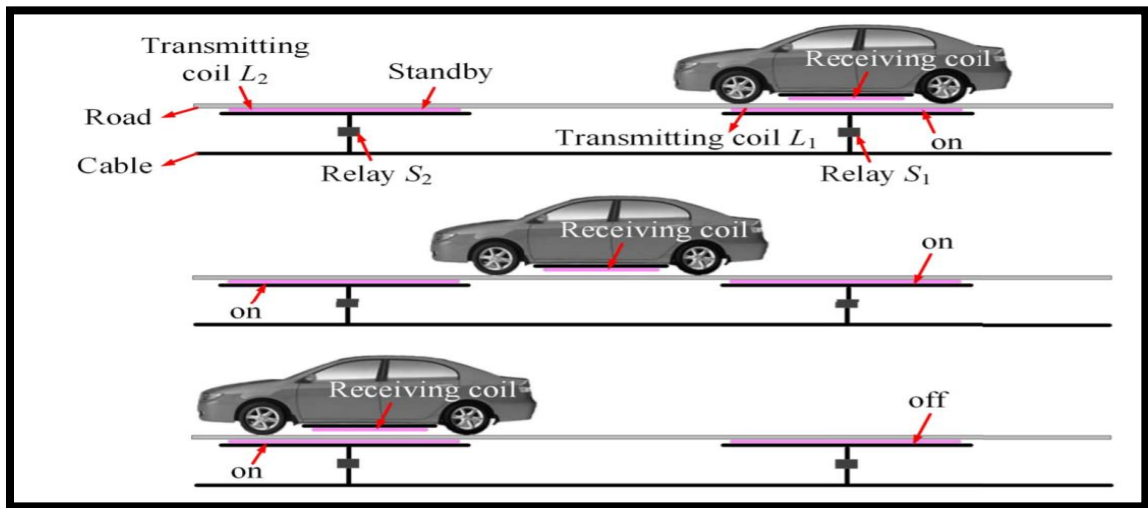


Fig 9: Selective Switch turn on/off for dynamic charging [31]

2.8 Cost estimation:

Cost plays a vital role in design and implementation. Comparing the cost of HEV, PHEV, OLEV, and PEV shows that the cost for OLEV is higher than the PHEV but less than the PEV [48]. Table 3 below shows the result of the study, the research is conducted with the information constructed in Seoul, Korea vehicle with an IC engine). The infrastructure is constructed in Seoul, Korea [48]

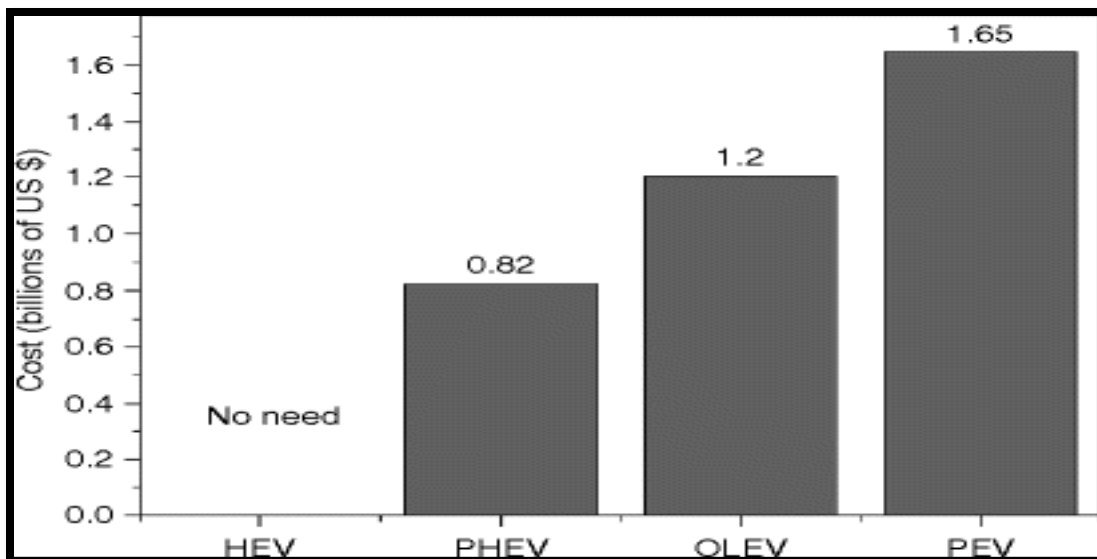


Fig 10: Comparison of the cost for infrastructure for PEV (plug-in all battery electric vehicle), OLEV, PHEV (plug-in hybrid electric vehicle), and HEV (hybrid electric vehicle).

As shown in the table below, the operating cost of OLEV, which is primarily the electricity cost, is estimated to be only 31% of cars that use gasoline [42] vehicles should be less than that of the hybrid cars and even regular cars with IC engines when they are produced in economical lot sizes.

Energy consumption costs (Driving distance: 13,286 km per year)					
Type	Energy consumption per year			Total energy cost (\$/year)	Reduced energy cost (\$/year)
	Gasoline (L)	LPG (L)	Electric (kWh)		
Gasoline	874			1,254	–
OLEV			4,429	391	863
HEV	624			895	360
HEV (LPG)		746		639	616
PHEV	312		1,536	568	686
PEV			3,126	276	979

Table 4: The manufacturing cost of OLEV passengers [42].

2.9 Intelligent Traffic Management

Mobility is ingrained in modern life; intelligent traffic management systems are a collection of services and technology linked to various modes of transportation and traffic control software. The most common applications of such systems are to provide residents with exact transportation information, shorten commute times, prevent downtime, and alleviate traffic congestion. It is designed to suit people's daily needs, serving thousands of users concurrently. On the other hand, vehicle operators can explore routes and schedules,

allowing them to coordinate their operations with their peers. Feedback control of the vehicle can provide an intelligent traffic management system.

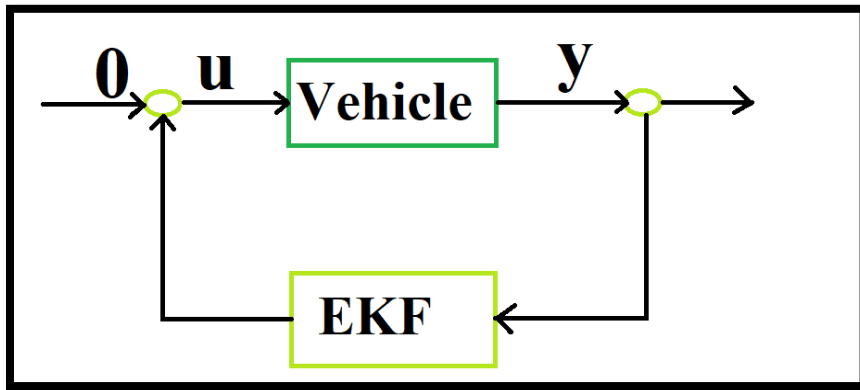


Fig 11: Feedback to maximize Inductive Power Transfer [38]

Dynamic IPT requires precise alignment of the road and vehicle coils to maximize power transfer. To facilitate this, we proposed an alignment system that combines data from a coil coupling sensor and a camera. The system is currently being simulated on straight and curved roads at various

Vehicle speed has considered incorporating the coupling sensor with data from a camera. The optic sensor detects the lane's lateral lines and estimates the lane's center position. While the inductance sensor is expected to be extremely precise (to the centimeter), the camera's precision is lower, in part because the transmitting coil's actual center may not be exactly in the center of the lane. However, optical information is required to estimate the displacement direction (to the left or the right), which is not available directly from the coil

sensor [38]. In this paper, we will use a feedback system to achieve the optimal speed while the vehicle follows the traffic.

Chapter 3 Misalignment of Dynamic Charging

Dynamic Electric vehicle charging efficiency considerably depended on the alignment of the transmitting coil and the receiving coil, and this chapter will delineate the calculation of mutual induction, charging design, and misalignment for a single vehicle.1

Fundamentals of Design Analysis for inductive Power transfer

The resonance inductive WPT operating principle is based on Amperes Law and Faradays Law. The HFAC signal passing through the primary winding produces a time-varying magnetic field (Ampere's law). The resultant magnetic flux is proportional to the Permeability of free space, the number of turns, and the current flowing through it. The time-varying magnetic flux induces an electric current in the secondary winding (Faraday's Law).

3.1.1 Basic equations for Power transformer

A generic model of a magnetic resonance-based system is shown in the figure below

$$\sum B^T \Delta l = \mu_0 I N p \quad (1)$$

$$E = -N_s \frac{d\phi_B}{dt} \quad (2)$$

where B^T , μ_0 , Δl , E , and ϕ_B represents magnetic flux density, the permeability of free space, length of the conductor, induced voltage, and magnetic flux respectively. N_p and N_s indicate the number of primary and secondary turns.

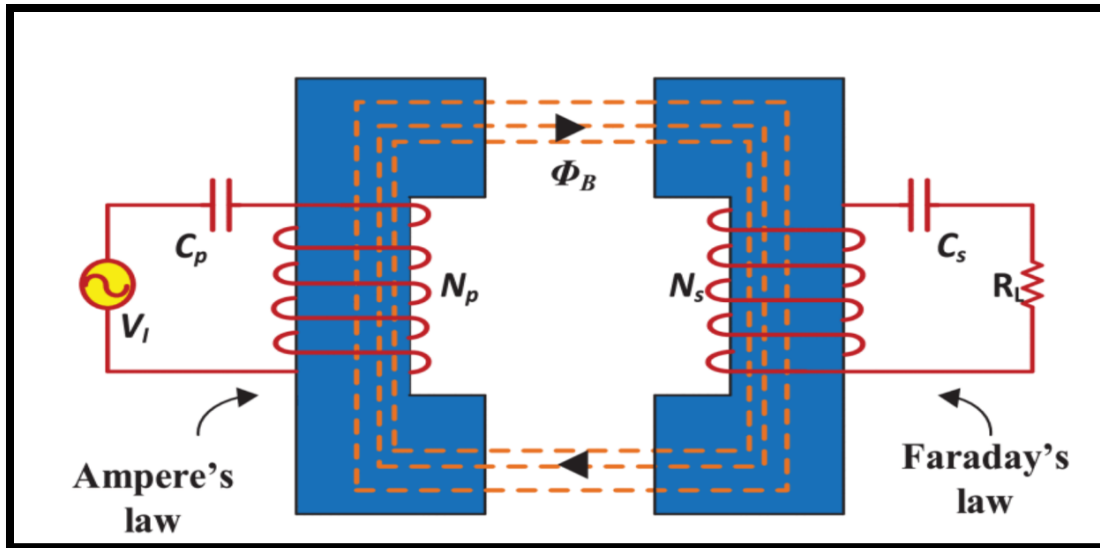


Fig 12: Generic Diagram of WPT [42]

3.2 Coil alignment for Power transfer

Coil orientation is a key parameter in the design of inductively coupled systems. The rate of change of power coupled across the inductive link when the RX coil is displaced from the ideal coaxial orientation is evaluated by the study of the two following forms of misalignment:

1) Lateral Misalignment: In lateral misalignment, a pair of TX(which is the primary or stationary coil) and RX coupled coils are situated in parallel planes, separated by a distance, and their centers are displaced by a distance.

2) Angular Misalignment: In angular misalignment, the plane of the RX(moving or dynamic coil) coil is tilted to form an angle and the axis of one coil passes through the center of the other coil.

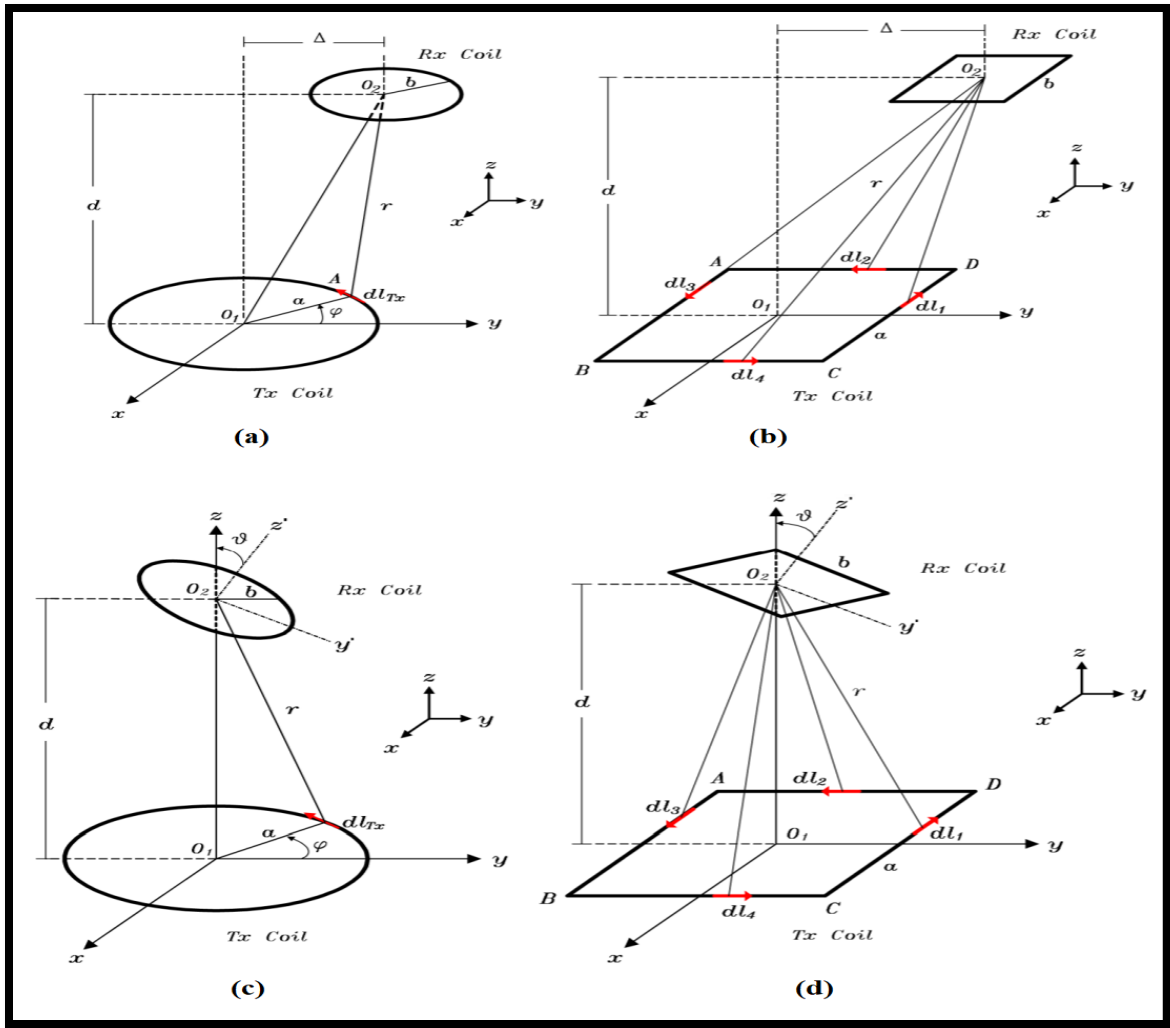


Fig 12: lateral and angular misalignment [43]

3.3 Mutual induction calculation

The computation of mutual inductance between coils that are misaligned has been extensively researched. The problem of coupler misalignment in WPT systems has also been investigated, and this requires the computation of mutual inductance between the couplers. WPT systems use a variety of coupler forms to achieve their mutual inductance, which is dependent on the shapes and orientations of the two coils adjacent to each other.

The mutual inductance depends on the shape and position of the two coils fig 20. Research [58] showed filamentary circular coils and cylindrical helix coils and used Neumann's formula to obtain the formulas for mutual inductance of two coils with misalignment.

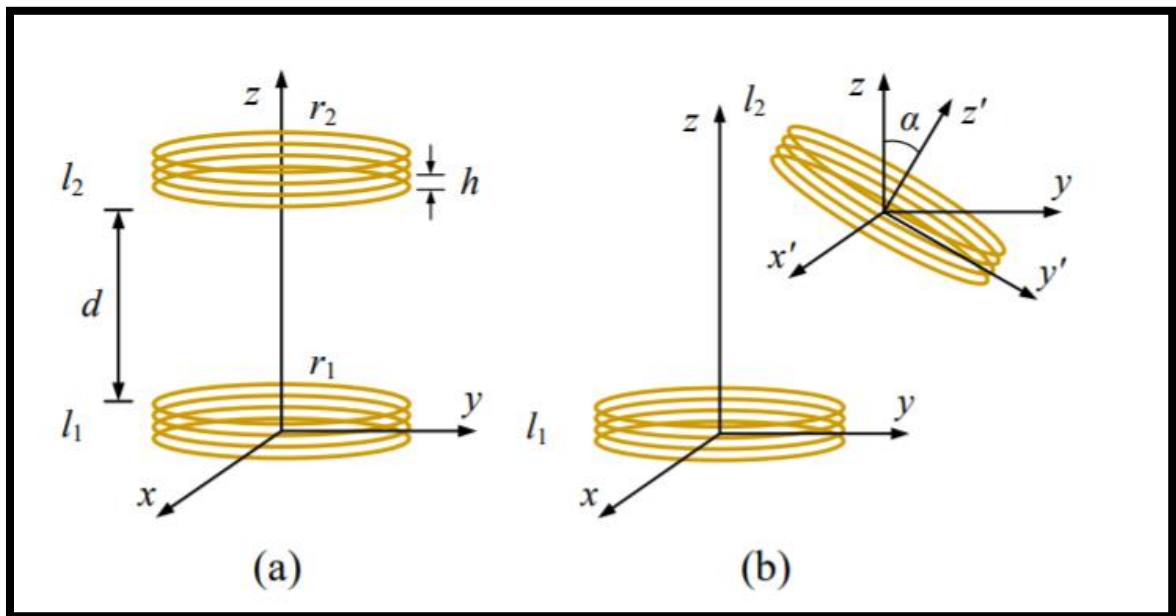


Fig 13: (a) Two coaxial cylindrical helix coils. (b) Two cylindrical helix coils with lateral and angular misalignment [58].

3.4 Charging structure for dynamic online electric vehicle:

The result of the calculation is shown in fig 14. This paper will use the reference calculation to establish the dynamic charging behavior of the electric vehicle. The maximum efficiency for the dynamic power transfer occurs when the Primary coil and secondary coil are in completely in alignment as shown in the figure below. The total power consumption from the coil is dependent on the time and the speed of the electric vehicle also which is shown in the following chapter.

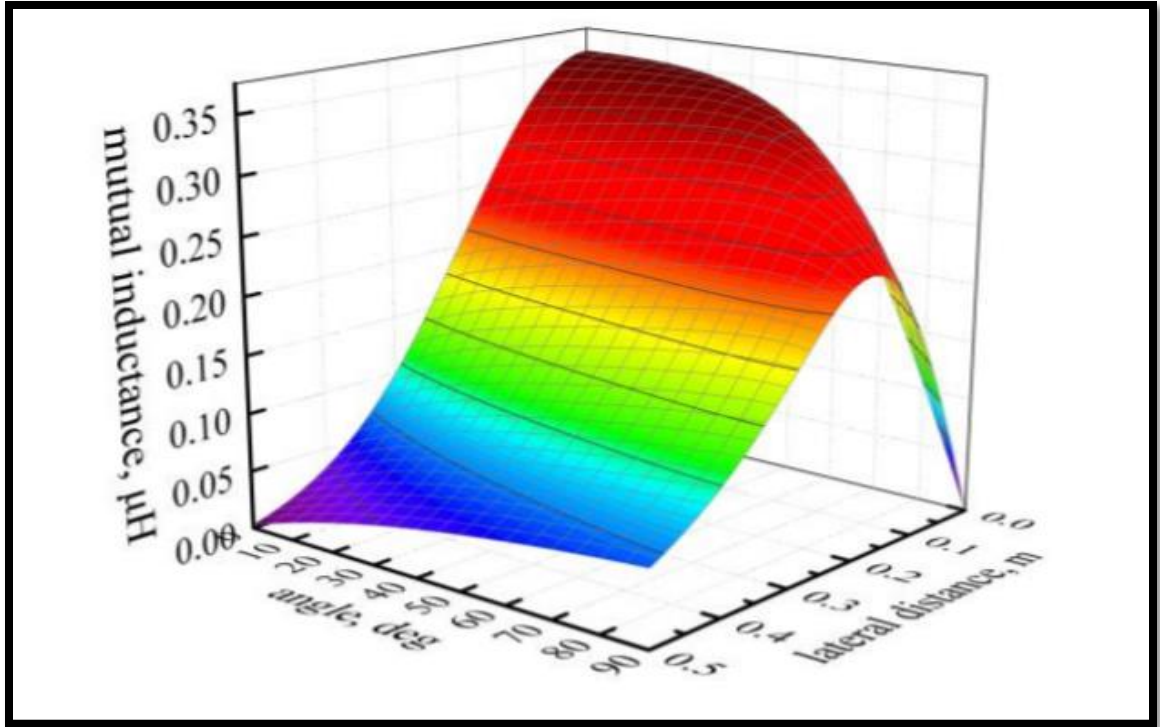


Fig 14: Lateral and angular misalignment output curve [58]

3.5 Investigating Misalignment for one vehicle

Model without traffic [75]

U is the input representing a command acceleration, i.e., $u=a$

$$\dot{v} = u$$

$$\dot{x} = v$$

Vehicle Models with road load physics can be written as a force balance, i.e.

$$F = \frac{1}{2} C_D \cdot A_f \cdot \rho \cdot v^2 + C_{rr} \cdot m_v \cdot g + m_v \cdot a \quad (3)$$

$$= \alpha_1 \cdot v^2 + \alpha_2 + \alpha_3 \cdot u \quad (4)$$

This is related to power through the following relationships

$$P = \frac{W}{t}$$

$$P = T \cdot \omega = (F \cdot d) \cdot \omega \quad (5)$$

Where $d \equiv$ (radius of the vehicle's wheel) and $\omega \equiv$ (rotational speed of the wheel in radians per second)

One rotation of the wheel = 2π radians per rotation

Then this leads to $\frac{\omega}{2\pi}$ wheel rotation per second, and $\omega \equiv$ (rotational speed of the wheel) in radians per second.

$$P = F \cdot v$$

$$P = \alpha_1 \cdot v^3 + \alpha_2 \cdot v + \alpha_3 \cdot u \cdot v \quad (6)$$

Assume we are driving over a charger located at a distance x_c from the starting position,

i.e.

$x = 0$.

$$P_c = \alpha_4 \cdot e^{\alpha_5 |x - x_c|}$$

Net power at each time instance is P_n , were

$$P_n = P_c - P = -(\alpha_1 \cdot v^3 + \alpha_2 \cdot v + \alpha_3 \cdot u \cdot v) + \alpha_4 \cdot e^{\alpha_5 |x - x_c|} \quad (7)$$

$$E = E(0) + \int_0^t P_n(\tau) d\tau \quad (8)$$

Now we consider to discretizing the model,

Say $x_1 = v$ and $x_2 = x$. Then

$$X(k) = \begin{pmatrix} x_1(k) \\ x_2(k) \end{pmatrix} \quad (9)$$

$$x_1(k+1) = x_1(k) + u \cdot \Delta t$$

$$x_2(k+1) = x_2(k) + x_1(k) \cdot \Delta t$$

We can write a discretized state space equation as

$$\begin{aligned} X(k+1) &= \begin{pmatrix} 1 & 0 \\ \Delta t & 1 \end{pmatrix} \cdot X(k) + \begin{pmatrix} \Delta t \\ 0 \end{pmatrix} \cdot u(k) \\ &= A \cdot X(k) + B \cdot u(k) \\ y(k) &= X(k) \end{aligned} \quad (10)$$

Also, $E - E(0) = \sum_{k=0}^m P_n(x_2(k), x_1(k), u(k)) \cdot \Delta t$ where $p_n(x_1, x_2, u) = -(\alpha_1 \cdot v^3 + \alpha_2 \cdot v + \alpha_3 \cdot u \cdot v) + \alpha_4 \cdot e^{\alpha_5 |x - x_c|}$

We would like to generate a control sequence

$$u(k), u(k+1), \dots, u(k+N_p-1)$$

At is feasible and minimizes the cost function where N_p is the control horizon. The predicted

State and output evolutions are

$$X(k+1|k), X(k+2|k), \dots, X(k+N_p|k)$$

Using recursion for the discretized state-space system we have

$$X(k+1|k) = A \cdot X(k) + B \cdot u(k)$$

$$X(k+2|k) = A \cdot X(k+1|k) + B \cdot u(k+1) = A^2 \cdot X(k) + AB \cdot u(k) + B \cdot u(k+1)$$

⋮

$$X(k + N_p | k) = A^{N_p} \cdot X(k) + A^{N_p-1} B \cdot u(k) + \dots + B \cdot u(k + N_p - 1)$$

In matrix form, this is the following

$$\begin{pmatrix} X(k + 1 | k) \\ X(k + 2 | k) \\ \vdots \\ X(k + N_p | k) \end{pmatrix} = \begin{pmatrix} A \\ A^2 \\ \vdots \\ A^{N_p} \end{pmatrix} X(k) + \begin{pmatrix} u(k) \\ u(k + 1) \\ \vdots \\ u(k + N_p - 1) \end{pmatrix} \quad (11)$$

$$X = A \cdot X(k) + B \cdot U$$

Cost Function and Optimization Problem

Since we do not wish to penalize input acceleration commands for braking, i.e. $u(\cdot) < 0$, we introduce a modified U vector \hat{U}

$$\hat{U} = \max\{U, 0\}$$

So we seek to minimize the following cost function,

$$J(U) = \frac{1}{2} q_1 \cdot (E - E(0))^2 + q_2 \cdot (x_1 - x_1^{SP})^2 + \frac{1}{2} \dots + \hat{U}^T R \hat{U} \quad (12)$$

Where $(q_1, q_2) > 0$ are scalar weights and $R = R^T \geq 0$ a weighting matrix of appropriate dimension. The constant X_l^{SP} is based on the target speed of the route.

The optimization problem is to minimize J over the control horizon so $m \equiv N_p - 1$.

Then the minimization problem is constrained and can be written as

$$\begin{aligned}
 & \min J \\
 & u(.) \\
 \text{Sub to } & \begin{cases} 0 < X_{min} \leq x_{max} \\ b \\ b \\ b \\ u_{min} \leq u \leq u_{max} \end{cases} \\
 \frac{\partial Pn}{\partial x1} \Big|_{x1(k), x2(k), u(k)} &= -3\alpha_1 x1^2 - \alpha_2 + \alpha_3 \cdot u \\
 \\
 \frac{\partial Pn}{\partial x1} \Big|_{x1(k), x2(k), u(k)} &= \begin{cases} \alpha_4 \cdot e^{-\alpha_5 |x-xc|} \cdot (-\alpha_5); & x2 - xc \geq 0 \\ \alpha_4 \cdot e^{-\alpha_5 |x-xc|} \cdot (-\alpha_5); & x2 - xc < 0 \end{cases} \\
 \\
 \frac{\partial Pn}{\partial x1} \Big|_{x1(k), x2(k), u(k)} &= -\alpha_3 \cdot x1 \tag{13}
 \end{aligned}$$

This chapter provides the background and calculation for each charging station and their behavior based on physical alignment. The characteristic of the misalignment is shown in figure 14. While we consider multiple charging stations a similar curve is seen which is shown in chapter 4.

Chapter 4. Simulation setup and result

In this chapter, the simulation setup and findings will be discussed. In our simulation set, up we have 10 charging stations for our controlled vehicle and the starting position is 200 m. Each charging station is 200m apart from the previous one. It also proposes a charging in fracture consideration for Maverick shuttle for Minnesota State University Mankato

4.1 Dynamic charging with one controlled vehicle and one vehicle in the front

Primarily we tried with a single controlled vehicle and another uncontrolled vehicle with random acceleration in front of our controlled vehicle. Our controlled vehicle is charging dynamically and the only constrain is that it will maintain an optimal speed without running into the vehicle in front of it, see appendix A for implementation details.

Figure 15 shows the energy consumed by the controlled vehicle during the time. Here we consider only one vehicle which is traveling in a linear direction and there are no constrain on the vehicle. That means this is the only vehicle traveling in the direction and there is no other vehicle present at this time on the road. The vehicle is consuming energy while it is traveling. The small bumps on the line graph mean that the vehicle is getting energy dynamically via magnetic coupling.

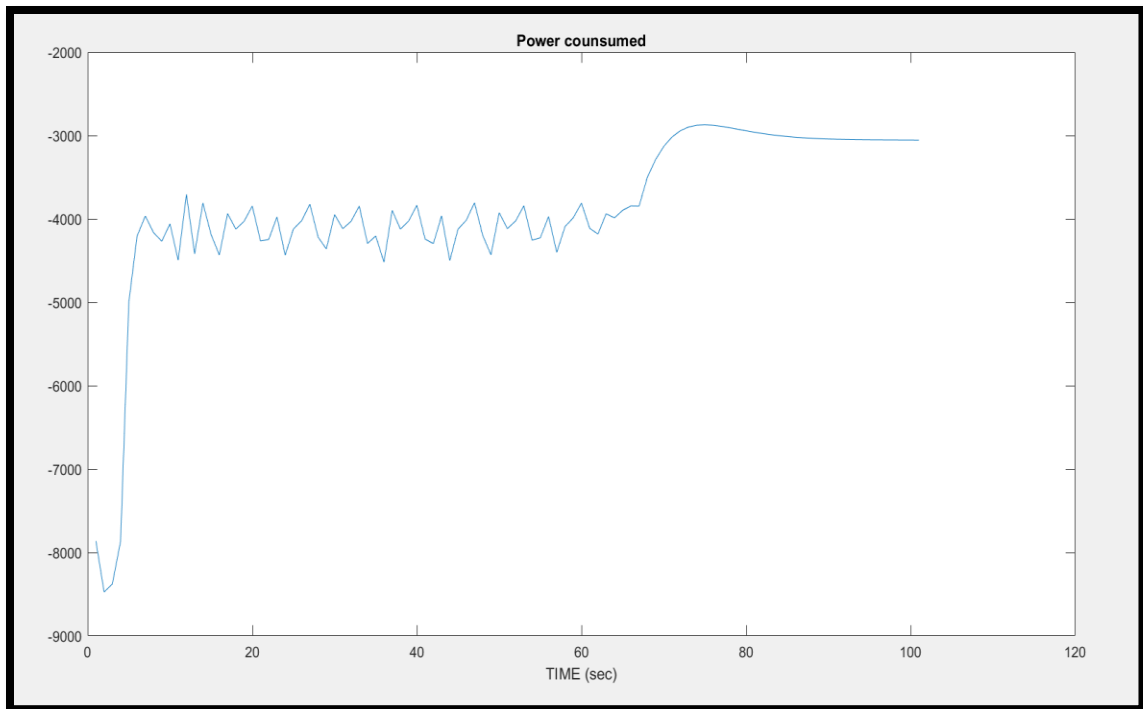


Fig 15: Energy consumed by the controlled vehicle while traveling.

Here now we consider two vehicles travelling in the same direction. One is our controlled vehicle(blue) and another is an uncontrolled vehicle. Figure 16 below shows (figure on the top) that the vehicle in front(green) is traveling almost at a constant velocity since we are using a random acceleration (positive and negative acceleration). Our controlled vehicle has only one constraint, it will not run into the vehicle in front of it and also change dynamically. From the figure, we can see the controlled vehicle is trying to maintain a constant velocity, and the distance traveled by the two vehicles is also shown. During the time interval of the simulation, the controlled vehicle never crossed the traffic vehicle, besides it tried to maintain a constant velocity. Which delineates that the controlled vehicle is behaving exactly we expected it to behave. The vehicle distance travel also shows that the controlled vehicle is maintaining to travel the given distance during the time of

simulation in a linear manner, and following the traffic vehicle without causing any traffic problem.

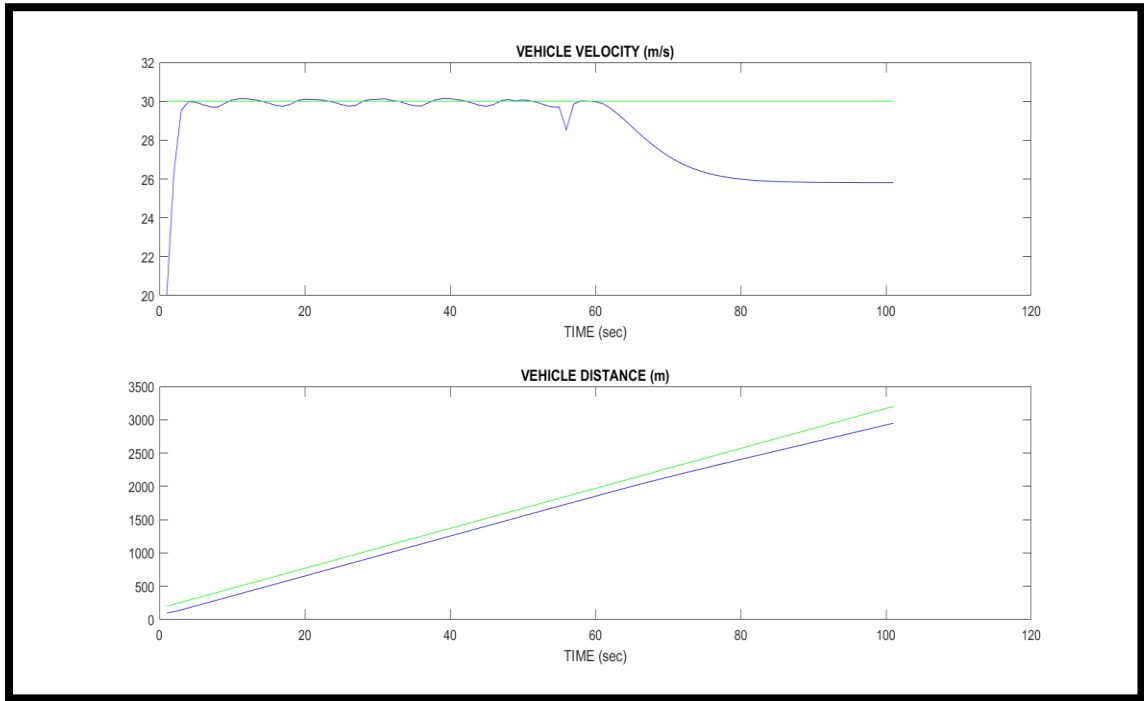


Fig 16: Velocity of controlled vehicle and vehicle in front(top), and distance traveled by the controlled vehicle in the front.

Fig 17 shows the controlled vehicle acceleration(top) and the mutual distance between the two vehicles. The acceleration declines rapidly after the control vehicle comes near the vehicle in the front, then increase to reach a linear distance. The response time of the controlled vehicle meets the expectation. The figure at the bottom shows that the mutual distance increases sharply after the controlled vehicle passed all of the charging stations and its speed declines sharply. This means that our vehicle is travelling while using the consuming energy it accruing during the travel.

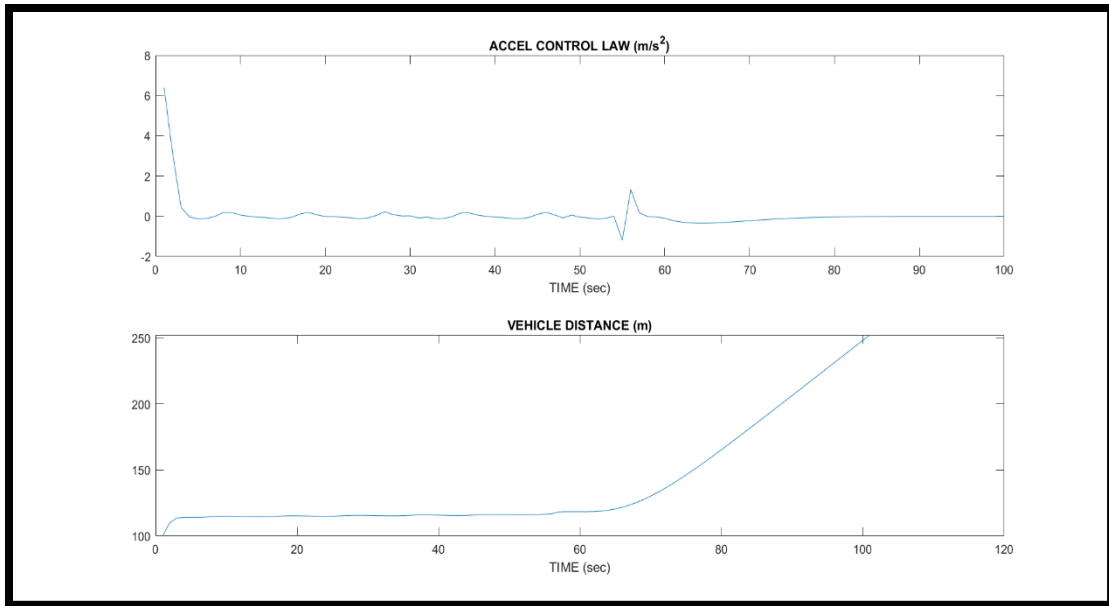


Figure 17: Acceleration of the controlled vehicle and the mutual distance between the two vehicles.

4.2 Control horizon, Time, and Power consumption of the controlled vehicle

Table 5 below shows the data for the controlled vehicle power consumption while we change the control horizon value for the calculation. The data shows that while the control horizon value is 3, we get the maximum power consumption.

Control horizon	Energy consumption (Watt seconds)	Time (seconds)
1	-2.78E+05	0.4657997
2	-4.15E+05	0.778921
3	-4.16E+05	1.6055393
4	-4.08E+05	2.533

5	-3.95E+05	4.4976
6	-3.79E+05	7.42
7	-3.62E+05	11.4632

Table 5: Power consumption for the controlled vehicle for different control horizon values and time for calculation (Matlab).

We have also investigated the time that needed for the different times are needed for the calculation in Matlab for different control horizons. The data shows that in Matlab, the time of calculation increases with the increase in the number of control horizons. However, if we consider the best energy consumption compared to the calculation time required, then control horizon values 3 and 4 provide us with the best result.

4.3 Dynamic charging with one controlled vehicle and one vehicle in the front and one in back

Later we used another constrain on our controlled vehicle. We added a vehicle behind and kept the vehicle in front as before. The condition is if the vehicle in the back comes closer and the distance between the controlled vehicle and the vehicle behind is less than or equal to 3 meters (about 8feet), then the controlled vehicle will check its distance between the vehicle in the front. If the distance between the controlled vehicle and the vehicle in the front is more than 3 meters then it will accelerate. However, the controlled vehicle must be at least 3meter behind the vehicle in the front. See appendix B for implementation details.

Fig 18 below shows the Power consumption by the controlled vehicle while moving. In this figure, energy consumption is less linear than energy consumption when we consider only a single vehicle with no traffic. This validates our expectation, since this time the controlled vehicle not only charging only, but it is accelerating and decelerating to maintain the distance from the traffic vehicle. Because of this acceleration and deceleration, the energy transfer is also varying.

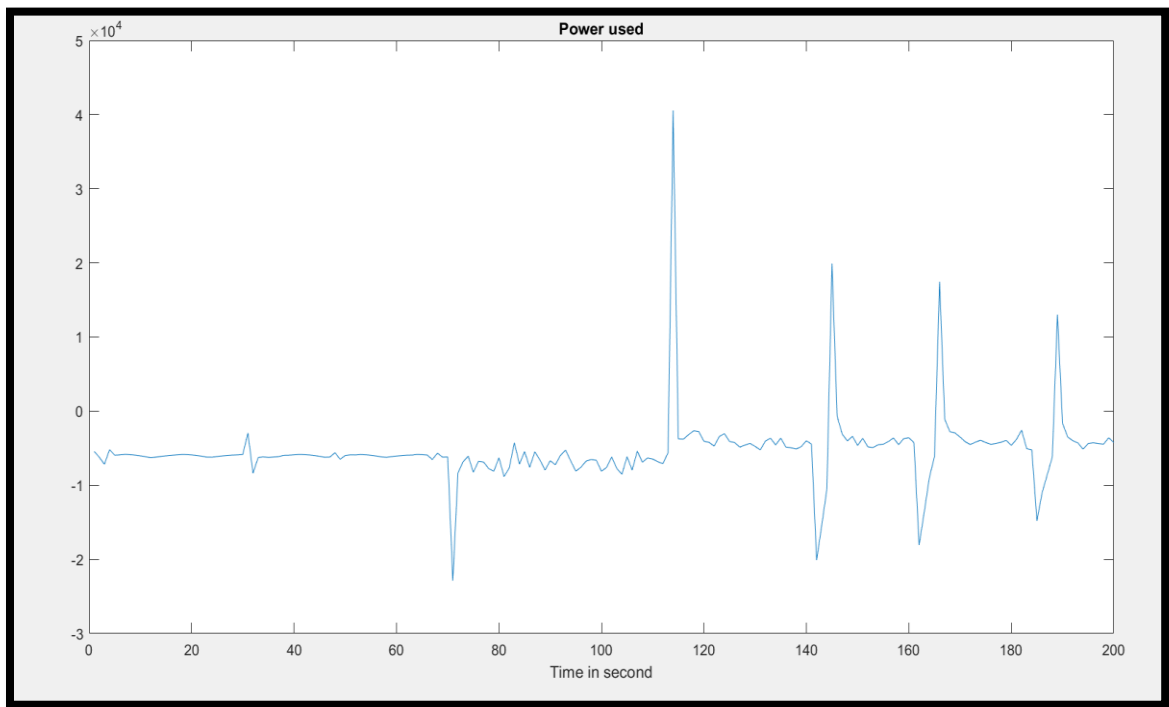


Fig 18: Power consumption by the controlled vehicle

Figure 19 below shows the velocity of the controlled vehicle (blue), the vehicle in the front, and the vehicle in the back. The vehicle in the back is running 3meter/second higher speed than the controlled vehicle, which will help us to see how the controlled vehicle behaves when the vehicle behind comes close to it. We have set a value of 3 meters as a safe distance, and our controlled vehicle will try to maintain this distance from the vehicle in the front

and the vehicle in the back as well. The controlled vehicle increases its velocity when the vehicle behind crosses the safe distance (3 meters is set). It tries to avoid collision by speeding up from the vehicle behind. However, as soon as it reaches the minimum safe distance between the vehicle in the front it decreases the speed. The figure also shows the 3-vehicle travel distance below. Since we did not put any constrain on the vehicle behind us, it crosses the constrain vehicle and the vehicle in the front. However, the controlled vehicle always stays behind the vehicle in the front by maintaining the minimum distance. Vehicle distance shows that the vehicle from behind cross the control vehicle (red cross blue). However, the control vehicle reduces the distance with the vehicle in the front in the beginning and maintains the distance (blue lines follow the green line) closely during the entire time.

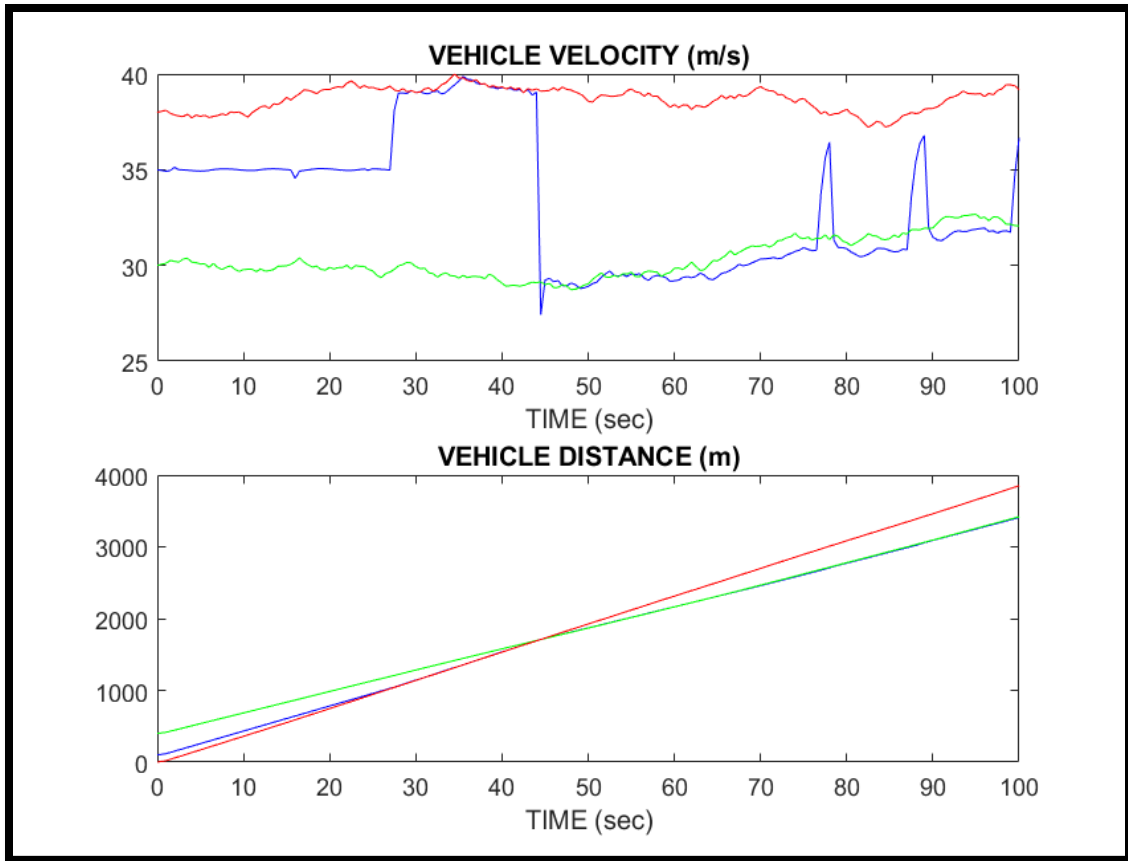


Fig 19: Vehicle velocity and traveling trajectory

Figure 20 shows the acceleration and deceleration of the controlled vehicle to keep the traffic moving without collision. It also shows the mutual distance between the vehicle in the front (green), which shows the mutual distance decreased primarily, and later the controlled vehicle tried to maintain a constant mutual distance. The red line is the mutual distance between the controlled vehicle and the vehicle in the back. In the beginning, the mutual distance increased from negative to zero, between 28 to 45 seconds the controlled vehicle tried to maintain a constant mutual distance before it crossed the safe distance with the vehicle in the front. After a certain point, the vehicle behind crossed the controlled vehicle since we did not put any constraint on it to simulate the result.

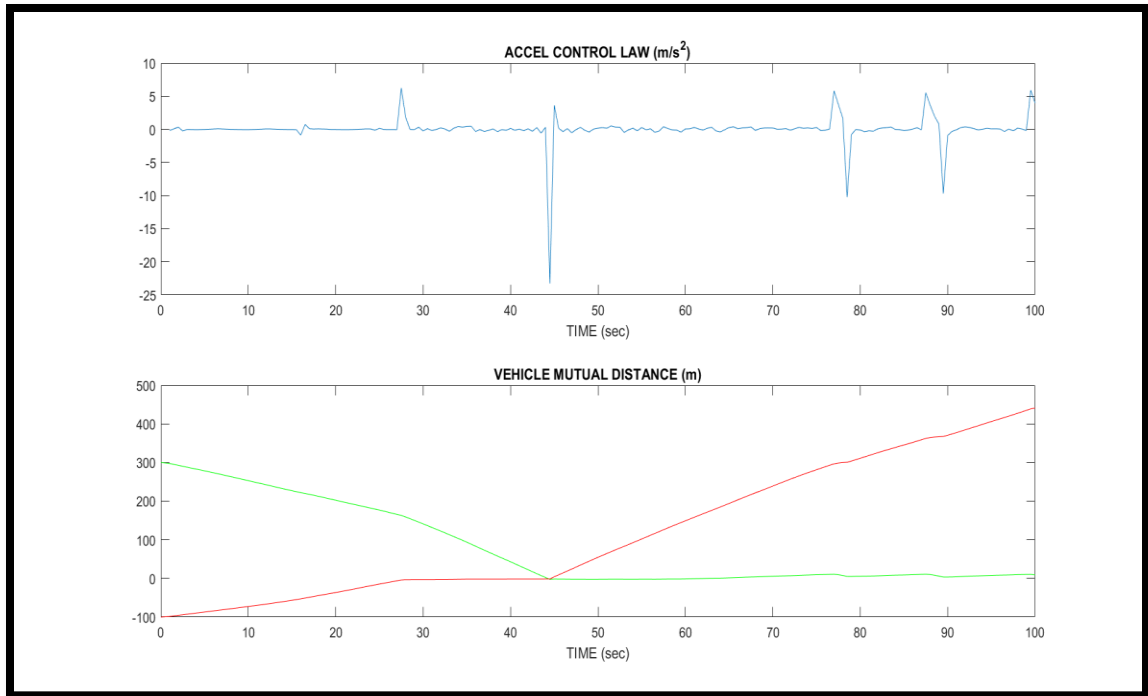


Fig 20: Controlled vehicle acceleration and mutual distance

4.4 Proposed Dynamic Electric Vehicle infrastructure for Maverick Shuttle

The energy consumption, while the vehicle is on move, is different from static wireless charging. The figure below is the finding of research at KAIST [74].

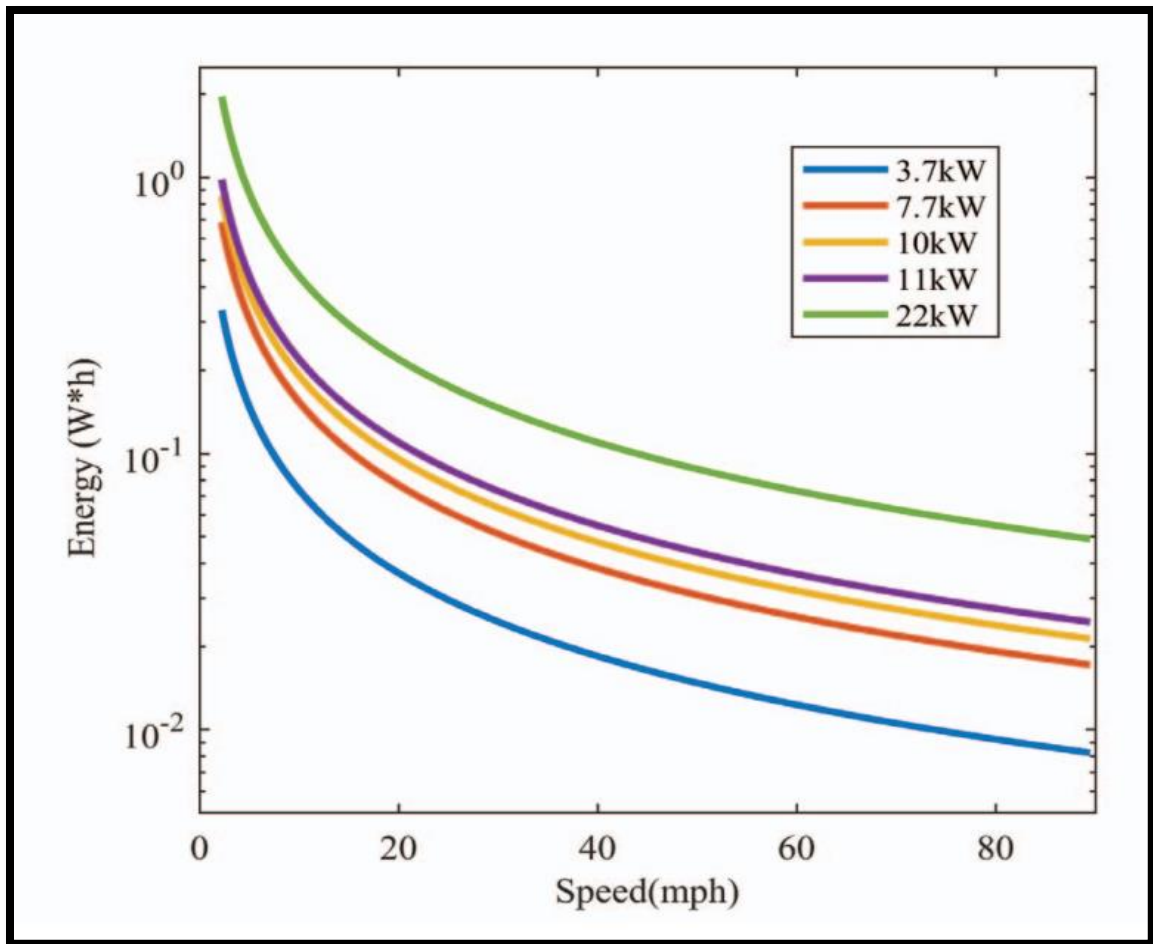


Fig 21: Energy transfer per coil vs speed [74]

Case 1: if the vehicle is static at a traffic light then the charging rate is about 1KWh which will drastically increase the energy transfer.

Case2: if the vehicle is running at 40 miles/hour and consuming at the rate of 22KWh then it can complete the complete route without making any stop and the energy at the starting and end of the journey will be conserved. The complete description is below with coil number consideration.

Case3: If the vehicle is traveling at 60 mph then the number of coils needed or at the current energy conversion rate makes it impossible to establish at the current time.

A typical light-duty EV uses .23KWh/mile. The paper provides a coil length of 1.6 meters and a minimum distance between two coils must be 81cm. If we use a single coil with this minimum clearance distance, we can maximum place about 751 coils in 1 mile. However, using bunch coil technology [74] a maximum of 1005 coils can be incorporated.

Now if the car is traveling 22KWh, we will need about 1000 coils to provide the needed power. However, we did not consider that the vehicle can stop in front of the traffic light which will sharply reduce the charging time.

Cost calculation and Prediction for MNSU bus route

To realize these benefits, sufficient wireless power transmitters need to be installed under the road surface. The initial investment in the wireless power transmitter infrastructures is high and depends on the number of wireless power transmitters installed. Therefore, to determine the appropriate investment in the wireless power transmitter infrastructures, the following issues need to be considered:

1. the number of wireless power transmitters to be installed on the route
2. the locations of the wireless power transmitters;
3. the length of inductive cable required for each wireless power transmitter

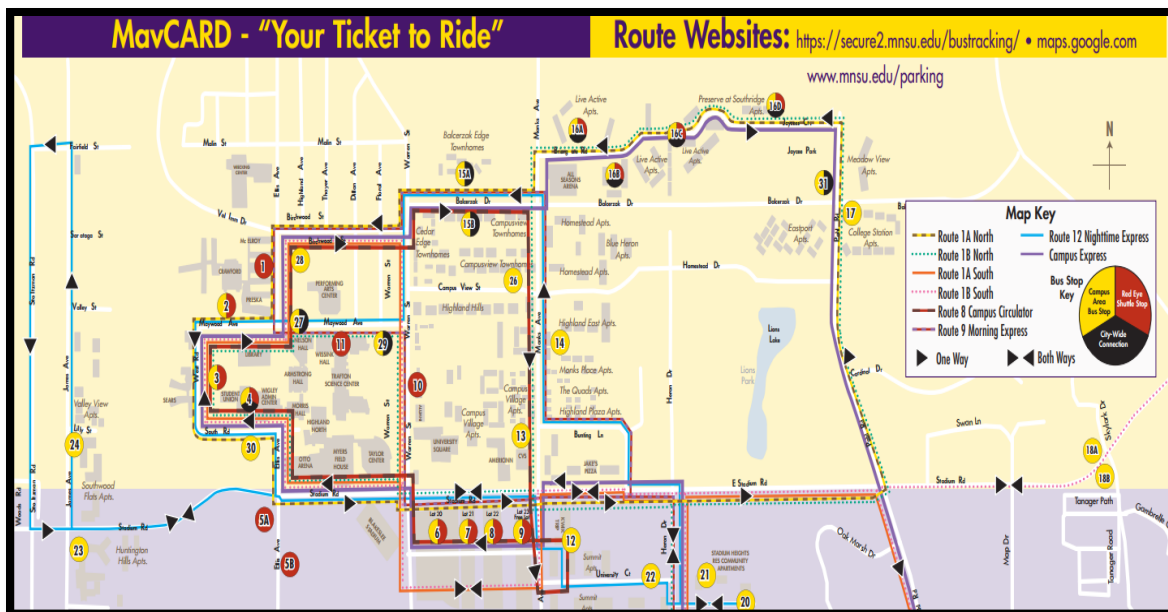


Fig 22: MNSU proposed Dynamic Electric Vehicle route

Figure 22 shows the proposed bus route where the dynamic charging station can be installed and the bus can run in a loop without the need for any external source of fuel. In the future, if we can implement a dynamic charging station in this traffic loop, then the MNSU school bus will be able to provide continuous service for students without stopping for fuel. The energy used to drive the bus and energy consumed from the power transfer from the pads will conserve and a net-zero energy balance can be achieved.

5. Research Findings and future suggestions

5.1 Findings:

The simulations represent the resulting trajectory of a controlled vehicle under various constraints countering and a finite timeline. The discretized dynamics have an iteration interval of one second. Figure 15 shows that instantaneous power is computed at discrete time steps based on the solution of the finite horizon optimal control posed in chapter 3. The bumps in the plot are induction of the vehicle encountering periodic charging pads. During these encounters, the vehicle velocity solution tends to accelerate the vehicle toward the charging pad and then decelerate once past the pad. This cyclic behavior indicated the power transfer advantage for the vehicle in close proximity to the charging pad. Without the constraints associated with maintaining traffic flow, the optimization solution would likely yield much more dramatic acceleration and deceleration events around the charging pads. Aside from the initial large power draw (due to acceleration), the simulation results indicate a reasonable balance of power draw and delivery throughout the entire timeline. Figure 16 shows the changes in the controlled vehicle velocity and relative distance from the traffic vehicle. The traffic vehicle is constrained to move at a constant velocity. The controlled vehicle trajectory solution tracks the traffic vehicle velocity until there are no additional charging pads in the roadways, after which the two vehicles diverge due to the controlled vehicle decelerating. Here the controlled vehicle can maintain relative speed and distance from the traffic while encountering the charging pads, however, once the charging pads are behind both vehicles, the controlled vehicle trajectory

solution tends toward penalizing the distance from the last charging pad. Figure 17 shows similar results but specific to the acceleration of the controlled vehicle.

5.2 Future Work

This paper did not incorporate the total charge prediction in complying with the road traffic condition. As mostly the road traffic is uncertain and even the data to make it predictable is a concern of security was a hinder toward drawing a complete calculation. However, in the future, if we can find a secure way for dynamic road traffic prediction and condition then this paper can provide the stepping stone to make the road traffic and electric vehicle charging for unmanned electric vehicles and will be able to draw the complete calculation.

Appendix A:

```
function f=charge(x)
```

```
    global X bigA bigB alpha1 alpha2 alpha3 alpha4 alpha5 x_sp xc Np q1 q2 R XT
    spdTarget
```

```
    bX = bigA*X + bigB*x;
```

```
    tP = 0;
```

```
    for i=1:Np
```

```
        P(i) = (alpha1*bX(2*i-1, 1)^3 + alpha2*bX(2*i-1, 1) + alpha3*bX(2*i-1, 1)*x(i));
```

```
        for k=1:length(xc)
```

```
            P(i) = P(i) - alpha4*exp(-alpha5*abs(bX(2*i, 1)-xc(k)));
```

```
        end %% k
```

```
        tP = tP + P(i);
```

```
    end
```

```
    se = bX(1:2:2*Np-1, 1)-spdTarget*ones(Np,1);
```

```
    te = bX(2:2:2*Np, 1)-XT(2, :, 1)*ones(Np,1);
```

Appendix B:

```
%% start the evolution with the initial condition on X and evolve one step each iteration
```

```
Xs = X; %% save the evolution
```

```
xtraffic = XT;
```

```
x_infront=zeros(2,100,2);
```

```
for i=1:t_iteration
```

```
    opt = optimset('MaxFunEvals',2e4,'MaxIter',2e4);
```

```
    %%[x fval] = fminsearch ( list(charge, X, alpha1, alpha2, alpha3, alpha4, alpha5, x_sp,
xc, Np, bigA, bigB, q1, q2, R, XT) , ones(Np,1), opt)
```

```
    %%[fopt, xopt, gopt] = optim (list(chargeCost, X, alpha1, alpha2, alpha3, alpha4,
alpha5, x_sp, xc, Np, bigA, bigB, q1, q2, R, XT), "b", accel_1, accel_u, ones(Np,1))
```

```
    xopt = fminsearch(@charge,ones(Np,1),opt);
```

```
    my_u(i) = xopt(1); %% keep the first input and discard the rest
```

```

dist(1) = xtraffic(2, i, 1) - Xs(2, i);
dist(2) = xtraffic(2, i, 2) - Xs(2, i);

Xs(:,i+1) = A*Xs(:,i) + B*my_u(i);

if ((dist(1) < distTarget) & (dist(2) > -distTarget))
    spdTarget = xtraffic(1,i,1);
elseif (dist(1) < distTarget)
    spdTarget = xtraffic(1,i,1);
elseif (dist(2) > -distTarget)
    spdTarget = xtraffic(1,i,2);
else
    spdTarget = spdBase;
end

X = Xs(:,i+1);

for j=1:2
    xtraffic_a = (0.5 - rand()); %% accel
    xtraffic(1,i+1,j) = xtraffic(1,i,j) + xtraffic_a*dt; %% changing speed random
    % xtraffic(1,i+1,j) = xtraffic(1,i,j) + sign(x_sp - xtraffic(1,i,j)) * xtraffic_a;
    xtraffic(2,i+1,j) = xtraffic(1,i,j)*dt+xtraffic(2,i,j); %% sum of the speed
    x_infront(1,i+1,j)=xtraffic_a+x_infront(2,i,j);

```



```
x_infront(2,i+1,j)=x_infront(2,i)+x_infront(1,i,j);  
end %j  
  
XT = xtraffic(:,i+1);  
  
i * dt  
end %% i
```

Bibliography

- [1] <https://www.earthobservatory.nasa.gov/features/CarbonCycle/page5.php>
- [2] <https://www.eia.gov/environment/emissions/carbon>
- [3] <https://www.iea.org/reports/tracking-transport-2020>
- [4] <http://www.historywebsite.co.uk/genealogy/Parker/ElwellParker.htm>
- [5] <https://edison.rutgers.edu/bio-long.htm>
- [6] <https://www.iea.org/fuels-and-technologies/renewables>
- [7] <https://www.iea.org/reports/renewables-2020>
- [8] Subotic, Ivan et al. "Single-Phase On-Board Integrated Battery Chargers for EVs Based on Multiphase Machines." *IEEE Transactions on Power Electronics* 31 (2016): 6511-6523.
- [9] N. Bodo, E. Levi, I. Subotic, J. Espina, L. Empringham and C. M. Johnson, "Efficiency evaluation of fully integrated onboard EV battery chargers with nine-phase machines", *IEEE Trans. Energy Convers.*, vol. 32, no. 1, pp. 257-266, Mar. 2017.
- [10] Liang, Xiaodong and Muhammad Sifatul Alam Chowdhury. "Emerging Wireless Charging Systems for Electric Vehicles - Achieving High Power Transfer Efficiency: A Review." 2018 IEEE Industry Applications Society Annual Meeting (IAS) (2018): 1-14.
- [11] X. Liang and M. S. A. Chowdhury, "Emerging Wireless Charging Systems for Electric Vehicles - Achieving High Power Transfer Efficiency: A Review," 2018 IEEE Industry Applications Society Annual Meeting (IAS), 2018, pp. 1-14, doi: 10.1109/IAS.2018.8544484.

- [12] Tong, Minghao et al. "A Single-Phase On-Board Two-Stage Integrated Battery Charger for EVs Based on a Five-Phase Hybrid-Excitation Flux-Switching Machine." *IEEE Transactions on Vehicular Technology* 69 (2020): 3793-3804.
- [13] Han, Bing. "Electric Vehicle Energy Management Considering Stakeholders' Interest in Smart Grids." (2019).
- [14] Assadi, Seyed Amir et al. "Active Saturation Mitigation in High-Density Dual-Active-Bridge DC–DC Converter for On-Board EV Charger Applications." *IEEE Transactions on Power Electronics* 35 (2020): 4376-4387.
- [16] M. Yilmaz and P. T. Krein, "Review of battery charger topologies, charging power levels, and infrastructure for plug-in electric and hybrid vehicles," *IEEE Trans. Power Electron.*, vol. 28, no. 5, pp. 2151–2169, May 2013.
- [17] C. Shi, Y. Tang and A. Khaligh, "A single-phase integrated onboard battery charger using propulsion system for plug-in electric vehicles", *IEEE Trans. Veh. Technol.*, vol. 66, no. 12, pp. 10899-10910, Dec. 2017.
- [18] Assadi, Seyed Amir et al. "Active Saturation Mitigation in High-Density Dual-Active-Bridge DC–DC Converter for On-Board EV Charger Applications." *IEEE Transactions on Power Electronics* 35 (2020): 4376-4387.
- [19] Choi, Woo-Young et al. "High-Frequency-Link Soft-Switching PWM DC–DC Converter for EV On-Board Battery Chargers." *IEEE Transactions on Power Electronics* 29 (2014): 4136-4145.

- [20] C. Liu, C. Jiang and C. Qiu, "Overview of coil designs for wireless charging of electric vehicle," 2017 IEEE PELS Workshop on Emerging Technologies: Wireless Power Transfer (WoW), 2017, pp. 1-6, doi: 10.1109/WoW.2017.7959389.
- [21] Zamani, Mohammad et al. "A review of inductive power transfer for electric vehicles." 2019 International Conference on Electrical Engineering Research & Practice (ICEERP) (2019): 1-5.
- [22] Wang, Chwei-Sen et al. "Design considerations for a contactless electric vehicle battery charger." IEEE Transactions on Industrial Electronics 52 (2005): 1308-1314.
- [23] C. Qiu, K. Chau, C. Liu, W. Li and F. Lin, "Quantitative comparison of dynamic flux distribution of magnetic couplers for roadway electric vehicle wireless charging system", Journal of Applied Physics, vol. 115, no. 17, pp. 17-334, Feb. 2014.
- [24] Mahesh, Aganti et al. "Inductive Wireless Power Transfer Charging for Electric Vehicles—A Review." IEEE Access 9 (2021): 137667-137713.
- [25] Qiao, Qinyu et al. "Cradle-to-gate greenhouse gas emissions of battery electric and internal combustion engine vehicles in China." Applied Energy 204 (2017): 1399-1411.
- [26] Bagchi, Anindya Chitta et al. "Review and Comparative Analysis of Topologies and Control Methods in Dynamic Wireless Charging of Electric Vehicles." IEEE Journal of Emerging and Selected Topics in Power Electronics 9 (2021): 4947-4962
- [27] Li, Siqi and Chunting Chris Mi. "Wireless Power Transfer for Electric Vehicle Applications." IEEE Journal of Emerging and Selected Topics in Power Electronics 3 (2015): 4-17.

- [28] Wu, Hunter H. et al. "A High Efficiency 5 kW Inductive Charger for EVs Using Dual Side Control." *IEEE Transactions on Industrial Informatics* 8 (2012): 585-595.
- [29] S. Lukic and Z. Pantic, "Cutting the Cord: Static and Dynamic Inductive Wireless Charging of Electric Vehicles," in *IEEE Electrification Magazine*, vol. 1, no. 1, pp. 57-64, Sept. 2013, doi: 10.1109/MELE.2013.2273228.
- [30] Ning, Puqi et al. "A compact wireless charging system for electric vehicles." 2013 *IEEE Energy Conversion Congress and Exposition* (2013): 3629-3634.
- [31] X. Zhang, Z. Yuan, Q. Yang, Y. Li, J. Zhu and Y. Li, "Coil Design and Efficiency Analysis for Dynamic Wireless Charging System for Electric Vehicles," in *IEEE Transactions on Magnetics*, vol. 52, no. 7, pp. 1-4, July 2016, Art no. 8700404, doi: 10.1109/TMAG.2016.2529682.
- [32] Babic, Slobodan et al. "VALIDITY CHECK OF MUTUAL INDUCTANCE FORMULAS FOR CIRCULAR FILAMENTS WITH LATERAL AND ANGULAR MISALIGNMENTS." *Progress in Electromagnetics Research M* 8 (2009): 15-26.
- [33] Fotopoulou, Kyriaki and Brian W. Flynn. "Wireless Power Transfer in Loosely Coupled Links: Coil Misalignment Model." *IEEE Transactions on Magnetics* 47 (2011): 416-430.
- [34] Mude, Kishore Naik and Maria Teresa Outeiro. "Coil misalignment analysis under different radius of coil and wire for Wireless Power Transfer System." *IECON 2017 - 43rd Annual Conference of the IEEE Industrial Electronics Society* (2017): 5319-5323.
- [35] Chen, Weitong et al. "Cost-Effectiveness Comparison of Coupler Designs of Wireless Power Transfer for Electric Vehicle Dynamic Charging." *Energies* 9 (2016): 906.

- [36] Kongwarakom, Watcharet et al. "Analysis and Design of Wireless Charging Lane for Light Rail Transit." 2020 International Conference on Power, Energy and Innovations (ICPEI) (2020): 29-32.
- [37] Diep, Nguyen Thi et al. "Design and Analysis of Coupling System in Electric Vehicle Dynamic Wireless Charging Applications." 2019 IEEE Vehicle Power and Propulsion Conference (VPPC) (2019): 1-6.
- [38] Cirimele, Vincenzo et al. "Maximizing Power Transfer for Dynamic Wireless Charging Electric Vehicles." ApplePies (2016).
- [39] Lukic, Srdjan M. and Zeljko Pantic. "Cutting the Cord: Static and Dynamic Inductive Wireless Charging of Electric Vehicles." IEEE Electrification Magazine 1 (2013): 57-64.
- [40] Nguyen, Dinh Hoa. "Electric Vehicle – Wireless Charging-Discharging Lane Decentralized Peer-to-Peer Energy Trading." IEEE Access 8 (2020): 179616-179625.
- [41] Nakil, Pranav et al. "WIRELESS CHARGING LANE & STATION FOR E-VEHICLE." (2020).
- [42] Ma, Chengbin et al. "Wireless Charging of Electric Vehicles: A Review and Experiments." (2011).
- [43] Ghassemi, Afshin et al. "A Novel Mathematical Model for Infrastructure Planning of Dynamic Wireless Power Transfer Systems for Electric Vehicles." ArXiv abs/2107.11428 (2021): n. pag.
- [44] Debbou, Mustapha and Francois Colet. "Inductive wireless power transfer for electric vehicle dynamic charging." 2016 IEEE PELS Workshop on Emerging Technologies: Wireless Power Transfer (WoW) (2016): 118-122.

- [45] YILMAZ, Mustafa and Philip T. Krein. "Review of charging power levels and infrastructure for plug-in electric and hybrid vehicles." 2012 IEEE International Electric Vehicle Conference (2012): 1-8.
- [46] Jang, Young Jae. "Survey of the operation and system study on wireless charging electric vehicle systems." *Transportation Research Part C: Emerging Technologies* (2018): n. pag.
- [47] Choi, Su Y. et al. "Ultraslim S-Type Power Supply Rails for Roadway-Powered Electric Vehicles." *IEEE Transactions on Power Electronics* 30 (2015): 6456-6468.
- [48] Lee, Min Seok and Young Jae Jang. "Charging Infrastructure Allocation for Wireless Charging Transportation System." (2017).
- [49] Cannon, Benjamin L. et al. "Magnetic Resonant Coupling As a Potential Means for Wireless Power Transfer to Multiple Small Receivers." *IEEE Transactions on Power Electronics* 24 (2009): 1819-1825.
- [50] Jeong, Seungmin et al. "Design optimization of the OLEV system considering battery lifetime." 17th International IEEE Conference on Intelligent Transportation Systems (ITSC) (2014): 2492-2498.
- [51] Alwesabi, Yaseen et al. "A novel integration of scheduling and dynamic wireless charging planning models of battery electric buses." *Energy* 230 (2021): 120806.
- [52] Kalwar, Kafeel Ahmed et al. "Inductively coupled power transfer (ICPT) for electric vehicle charging – A review." *Renewable & Sustainable Energy Reviews* 47 (2015): 462-475.

- [53] Hasan, Mohammad Kamrul et al. "Review of electric vehicle energy storage and management system: Standards, issues, and challenges." *Journal of energy storage* 41 (2021): 102940.
- [54] Qiu, Chun et al. "Overview of wireless power transfer for electric vehicle charging." *2013 World Electric Vehicle Symposium and Exhibition (EVS27)* (2013): 1-9.
- [55] Sun, Longzhao et al. "A review of recent trends in wireless power transfer technology and its applications in electric vehicle wireless charging." *Renewable and Sustainable Energy Reviews* (2018): n. pag.
- [56] Jang, Young Jae et al. "System optimization of the On-Line Electric Vehicle operating in a closed environment." *Comput. Ind. Eng.* 80 (2015): 222-235.
- [57] Ko, Young Dae and Young Jae Jang. "The Optimal System Design of the Online Electric Vehicle Utilizing Wireless Power Transmission Technology." *IEEE Transactions on Intelligent Transportation Systems* 14 (2013): 1255-1265.
- [58] Chen, Zhibin et al. "Optimal deployment of charging lanes for electric vehicles in transportation networks." *Transportation Research Part B-methodological* 91 (2016): 344-365.
- [59] Zhang, Fan et al. "Literature review of electric vehicle technology and its applications." *2016 5th International Conference on Computer Science and Network Technology (ICCSNT)* (2016): 832-837.
- [60] Cheng, Ka Wai Eric. "Recent development on electric vehicles." *2009 3rd International Conference on Power Electronics Systems and Applications (PESA)* (2009): 1-5.

- [61] https://theicct.org/sites/default/files/publications/EV_cost_2020_2030_20190401.pdf
- [62] <https://www.iea.org/areas-of-work/programmes-and-partnerships/electric-vehicles-initiative>
- [63] <https://www.whitehouse.gov/briefing-room/statements-releases/2021/02/11/biden-harris-administration-launches-american-innovation-effort-to-create-jobs-and-tackle-the-climate-crisis/>
- [64] <https://www.whitehouse.gov/briefing-room/statements-releases/2021/03/31/fact-sheet-the-american-jobs-plan/>
- [65] Rim, Chun T. and Chris Mi. "History of RPEVs." (2017).
- [66] Ahmad, Aqueel et al. "A Comprehensive Review of Wireless Charging Technologies for Electric Vehicles." *IEEE Transactions on Transportation Electrification* 4 (2018): 38-63.
- [67] Machura, Philip and Quan Li. "A critical review on wireless charging for electric vehicles." *Renewable and Sustainable Energy Reviews* (2019): n. pag.
- [68] Mi, Chunting Chris et al. "Modern Advances in Wireless Power Transfer Systems for Roadway Powered Electric Vehicles." *IEEE Transactions on Industrial Electronics* 63 (2016): 6533-6545.
- [69] Choi, Su Yeon et al. "Trends of Wireless Power Transfer Systems for Roadway Powered Electric Vehicles." *2014 IEEE 79th Vehicular Technology Conference (VTC Spring)* (2014): 1-5.

- [70] Rajendran, Gowthamraj et al. "A comprehensive review on system architecture and international standards for electric vehicle charging stations." *Journal of energy storage* 42 (2021): 103099.
- [71] Machura, Philip and Quan Li. "A critical review on wireless charging for electric vehicles." *Renewable and Sustainable Energy Reviews* (2019): n. pag.
- [72] Jeong, Seungmin et al. "Economic Analysis of the Dynamic Charging Electric Vehicle." *IEEE Transactions on Power Electronics* 30 (2015): 6368-6377.
- [73] Kim, Jiseong et al. "Coil Design and Shielding Methods for a Magnetic Resonant Wireless Power Transfer System." *Proceedings of the IEEE* 101 (2013): 1332-1342.
- [74] Foote, Andrew et al. "Sizing dynamic wireless charging for light-duty electric vehicles in roadway applications." 2016 IEEE PELS Workshop on Emerging Technologies: Wireless Power Transfer (WoW) (2016): 224-230.
- [75] V. Winstead and A. Jemi (2022), "Receding Horizon Control for Wireless Charging Networks", Submitted to the 2022 IEEE International Conference on Electro-Information Technology (EIT), Mankato, USA.